

1 **Mitochondrial respiratory states and rates:**
2 **Building blocks of mitochondrial physiology**
3 **Part 1.** MitoEAGLE preprint 2018-02-22(28)
4

5 http://www.mitoeagle.org/index.php/MitoEAGLE_preprint_2018-02-08
6

7 Preprint version 28 (2018-02-28)

8 **MitoEAGLE Network**

9 Corresponding author: Gnaiger E

10 Contributing co-authors

11 Aasander Frostner E, Acuna-Castroviejo D, Ahn B, Alves MG, Amati F, Aral C,
12 Arandarčikaitė O, Bailey DM, Bakker BM, Bastos Sant'Anna Silva AC, Battino M, Beard
13 DA, Ben-Shachar D, Bishop D, Borutaitė V, Breton S, Brown GC, Brown RA, Buettner GR,
14 Burtscher J, Calabria E, Calbet JA, Cardoso LHD, Carvalho E, Casado Pinna M, Cervinkova
15 Z, Chang SC, Chaurasia B, Chen Q, Chicco AJ, Chinopoulos C, Clementi E, Coen PM, Collin
16 A, Collins JL, Crisóstomo L, Das AM, Davis MS, De Palma C, Dias TR, Distefano G,
17 Doerrier C, Drahota Z, Duchon MR, Ehinger J, Elmer E, Endlicher R, Fell DA, Ferko M,
18 Ferreira JCB, Filipovska A, Fisar Z, Fischer M, Fisher JJ, Fornaro M, Galkin A, Garcia-
19 Roves PM, Garcia-Souza LF, Genova ML, Giovarelli M, Gonzalo H, Goodpaster BH, Gorr
20 TA, Gourlay CW, Granata C, Grefte S, Haas CB, Haavik J, Han J, Harrison DK, Hellgren
21 KT, Hernansanz-Agustin P, Holland O, Hoppel CL, Houstek J, Hunger M, Iglesias-Gonzalez
22 J, Irving BA, Iyer S, Jackson CB, Jadiya P, Jang DH, Jansen-Dürr P, Jespersen NR, Jha RK,
23 Kaambre T, Kane DA, Kappler L, Karabatsiakos A, Keijer J, Keppner G, Klingenspor M,
24 Komlodi T, Kopitar-Jerala N, Krako Jakovljevic N, Kuang J, Kucera O, Labieniec-Watala M,
25 Lai N, Laner V, Larsen TS, Lee HK, Lemieux H, Lerfall J, Lucchinetti E, MacMillan-Crow
26 LA, Makrečka-Kuka M, Malik A, Markova M, Meszaros AT, Michalak S, Moiso N, Molina
27 AJA, Montaigne D, Moore AL, Moreira BP, Mracek T, Muntane J, Muntean DM, Murray AJ,
28 Nemeč M, Neuzil J, Newsom S, Nozickova K, O'Gorman D, Oliveira PF, Oliveira PJ,
29 Orynbayeva Z, Pak YK, Palmeira CM, Patel HH, Pecina P, Pelnena D, Pereira da Silva Grilo
30 da Silva F, Pesta D, Petit PX, Pichaud N, Piel S, Pirkmajer S, Porter RK, Pranger F,
31 Prochownik EV, Pulinilkunnit T, Puurand M, Radenkovic F, Radi R, Ramzan R, Reboredo P,
32 Renner-Sattler K, Robinson MM, Rohlena J, Ropelle ER, Røslund GV, Rossiter HB,
33 Rybacka-Mossakowska J, Saada A, Salvadego D, Sandi C, Scatena R, Schartner M,
34 Scheibye-Knudsen M, Schilling JM, Schlattner U, Schoenfeld P, Schwarzer C, Scott GR,
35 Shabalina IG, Sharma P, Sharma V, Shevchuk I, Siewiera K, Silber AM, Singer D, Smenes
36 BT, Soares FAA, Sobotka O, Sokolova I, Spinazzi M, Stankova P, Stier A, Stocker R,
37 Sumbalova Z, Suravajhala P, Swiniuch D, Tanaka M, Tandler B, Tepp K, Tomar D, Towheed
38 A, Tretter L, Trifunovic A, Trivigno C, Tronstad KJ, Trougakos IP, Tyrrell DJ, Urban T,
39 Valentine JM, Velika B, Vendelin M, Vercesi AE, Victor VM, Villena JA, Vogt S, Volani C,
40 Votion DM, Vujacic-Mirski K, Wagner BA, Ward ML, Watala C, Wei YH, Wieckowski MR,
41 Williams C, Wohlwend M, Wolff J, Wuest RCI, Zaugg K, Zaugg M, Zischka H, Zorzano A
42

43 Supporting co-authors:

44 Bernardi P, Boetker HE, Borsheim E, Bouitbir J, Calzia E, Coker RH, Dubouchaud H,
45 Durham WJ, Dyrstad SE, Engin AB, Gan Z, Garlid KD, Garten A, Haendeler J, Hand SC,
46 Hepple RT, Hickey AJ, Hoel F, Kainulainen H, Khamoui AV, Koopman WJH, Kowaltowski
47 AJ, Krajcova A, Lane N, Lenaz G, Liu J, Liu SS, Mazat JP, Menze MA, Methner A,
48 Nedergaard J, Oliveira MT, Pallotta ML, Parajuli N, Pettersen IK, Porter C, Salin K,
49 Sazanov LA, Skolik R, Sonkar VK, Swerdlow RH, Szabo I, Thyfault JP, Vieyra A
50
51

Updates and discussion:

http://www.mitoeagle.org/index.php/MitoEAGLE_preprint_2018-02-08

Correspondence: Gnaiger E

Chair COST Action CA15203 MitoEAGLE – <http://www.mitoeagle.org>

Department of Visceral, Transplant and Thoracic Surgery, D. Swarovski Research Laboratory, Medical University of Innsbruck, Innrain 66/4, A-6020 Innsbruck, Austria

Email: erich.gnaiger@i-med.ac.at

Tel: +43 512 566796, Fax: +43 512 566796 20

Contents**Abstract****Executive summary****1. Introduction** – Box 1: In brief: Mitochondria and Bioblasts**2. Oxidative phosphorylation and coupling states in mitochondrial preparations**

Mitochondrial preparations

2.1. Respiratory control and coupling

The steady-state

Specification of biochemical dose

Phosphorylation, P_{\gg} , and P_{\gg}/O_2 ratio

Control and regulation

Respiratory control and response

Respiratory coupling control and ET-pathway control

Coupling

Uncoupling

2.2. Coupling states and respiratory rates

Respiratory capacities in coupling control states

LEAK, OXPHOS, ET, ROX

2.3. Classical terminology for isolated mitochondria

States 1–5

3. Normalization: fluxes and flows*3.1. Normalization: system or sample*

Flow per system, I

Extensive quantities

Size-specific quantities – Box 2: Metabolic fluxes and flows: vectorial and scalar

3.2. Normalization for system-size: flux per chamber volume

System-specific flux, J_{V,O_2}

3.3. Normalization: per sample

Sample concentration, C_{mX}

Mass-specific flux, $J_{O_2/mX}$

Number concentration, C_{NX}

Flow per object, $I_{O_2/X}$

3.4. Normalization for mitochondrial content

Mitochondrial concentration, C_{mtE} , and mitochondrial markers

Mitochondria-specific flux, $J_{O_2/mtE}$

*3.5. Evaluation of mitochondrial markers**3.6. Conversion: units***4. Conclusions** – Box 3: Mitochondrial and cell respiration**5. References**

102 **Abstract** As the knowledge base and importance of mitochondrial physiology to human health
103 expands, the necessity for harmonizing nomenclature concerning mitochondrial respiratory
104 states and rates has become increasingly apparent. Clarity of concept and consistency of
105 nomenclature are key trademarks of a research field. These trademarks facilitate effective
106 transdisciplinary communication, education, and ultimately further discovery. Peter Mitchell's
107 chemiosmotic theory establishes the mechanism of energy transformation and coupling in
108 oxidative phosphorylation. The unifying concept of the protonmotive force provides the
109 framework for developing a consistent theory and nomenclature for mitochondrial physiology
110 and bioenergetics. Herein, we follow IUPAC guidelines on general terms of physical chemistry,
111 extended by considerations on open systems and irreversible thermodynamics. We align the
112 nomenclature and symbols of classical bioenergetics with a concept-driven constructive
113 terminology to express the meaning of each quantity clearly and consistently. In this position
114 statement, in the frame of COST Action MitoEAGLE, we endeavour to provide a balanced
115 view on mitochondrial respiratory control and a critical discussion on reporting data of
116 mitochondrial respiration in terms of metabolic flows and fluxes. Uniform standards for
117 evaluation of respiratory states and rates will ultimately support the development of databases
118 of mitochondrial respiratory function in species, tissues, and cells.

119

120 *Keywords:* Mitochondrial respiratory control, coupling control, mitochondrial
121 preparations, protonmotive force, oxidative phosphorylation, OXPHOS, efficiency, electron
122 transfer, ET; proton leak, LEAK, residual oxygen consumption, ROX, State 2, State 3, State 4,
123 normalization, flow, flux, O₂

124

125

126

127 **Executive summary**

128

129

130 1. In view of broad implications on health care, mitochondrial researchers face an
131 increasing responsibility to disseminate their fundamental knowledge and novel
132 discoveries to a wide range of stakeholders and scientists beyond the group of
133 specialists. This requires implementation of a commonly accepted terminology
134 within the discipline and standardization in the translational context. Authors,
135 reviewers, journal editors, and lecturers are challenged to collaborate with the aim
136 to harmonize the nomenclature in the growing field of mitochondrial physiology
and bioenergetics.

137

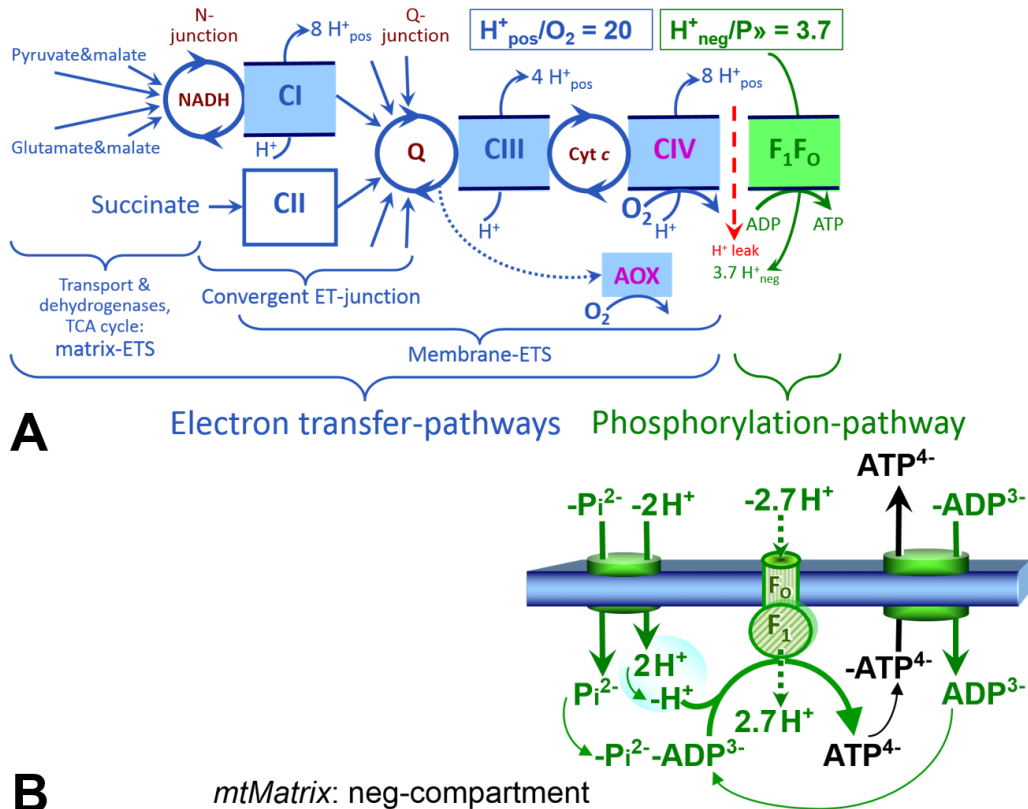
138 2. Aerobic energy metabolism in mammalian mitochondria depends on the coupling of
139 phosphorylation (ADP → ATP) to O₂ flux in catabolic reactions. In this process of
140 oxidative phosphorylation, coupling is mediated by translocation of protons
141 through respiratory proton pumps operating across the inner mitochondrial
142 membrane and generating or utilizing the protonmotive force measured between
143 the mitochondrial matrix and intermembrane compartment. Compartmental
144 coupling thus distinguishes vectorial oxidative phosphorylation from fermentation
as the counterpart of cellular core energy metabolism.

145

146 3. To exclude fermentation and other cytosolic interactions from exerting an effect on
147 mitochondrial metabolism, the barrier function of the plasma membrane must be
148 disrupted. Selective removal or permeabilization of the plasma membrane yields
149 mitochondrial preparations—including isolated mitochondria, tissue and cellular
150 preparations—with structural and functional integrity. Then extra-mitochondrial
151 concentrations of fuel substrates transported into the mitochondrial matrix, ADP,
ATP, inorganic phosphate, and cations including H⁺ can be controlled to determine
152 mitochondrial function under a set of conditions defined as coupling control states.

153
154
155
156
157

A concept-driven terminology of bioenergetics incorporates in its terms and symbols explicit information on the nature of respiratory states, that makes the technical terms readily recognized and easy to understand.



158
159
160
161
162
163
164
165
166
167
168
169
170
171
172
173
174
175
176
177
178
179

Fig. 1. The oxidative phosphorylation (OXPHOS) system. (A) The mitochondrial electron transfer system (ETS) is fuelled by diffusion and transport of substrates across the mtOM and mtIM and consists of the matrix-ETS and membrane-ETS. ET-pathways are coupled to the phosphorylation-pathway. ET-pathways converge at the N-junction and Q-junction. Additional arrows indicate electron entry into the Q-junction through electron transferring flavoprotein, glycerophosphate dehydrogenase, dihydro-orotate dehydrogenase, choline dehydrogenase, and sulfide-ubiquinone oxidoreductase. The dotted arrow indicates the branched pathway of oxygen consumption by alternative quinol oxidase (AOX). The H^+_{pos}/O_2 ratio is the outward proton flux from the matrix space to the positively (pos) charged compartment, divided by catabolic O_2 flux in the NADH-pathway. The $H^+_{neg}/P \gg 3.7$ ratio is the inward proton flux from the inter-membrane space to the negatively (neg) charged matrix space, divided by the flux of phosphorylation of ADP to ATP (Eq. 1). These are not fixed stoichiometries due to ion leaks and proton slip. (B) Phosphorylation-pathway catalyzed by the proton pump F₁F₀-ATPase (F-ATPase, ATP synthase), adenine nucleotide translocase, and inorganic phosphate transporter. The $H^+_{neg}/P \gg 3.7$ stoichiometry is the sum of the coupling stoichiometry in the F-ATPase reaction ($-2.7 H^+_{pos}$ from the positive intermembrane space, $2.7 H^+_{neg}$ to the matrix, *i.e.*, the negative compartment) and the proton balance in the translocation of ADP^{3-} , ATP^{4-} and P_i^{2-} . Modified from (A) Lemieux *et al.* (2017) and (B) Gnaiger (2014).

- 180 4. Mitochondrial coupling states are defined according to the control of respiratory oxygen
 181 flux by the protonmotive force. Capacities of oxidative phosphorylation and
 182 electron transfer capacities are measured at kinetically saturating concentrations of
 183 fuel substrates, ADP and inorganic phosphate, or at optimal uncoupler
 184 concentrations, respectively. Respiratory capacities are a measure of the upper
 185 bound of the rates of respiration, providing reference values for the diagnosis of
 186 health and disease, and for evaluation of the effects of **E**volutionary background,
 187 **A**ge, **G**ender and sex, **L**ifestyle and **E**nvironment (EAGLE).
- 188 5. Some degree of uncoupling is a characteristic of energy-transformations across
 189 membranes. Uncoupling is caused by a variety of physiological, pathological,
 190 toxicological, pharmacological and environmental conditions that exert an
 191 influence not only on the proton leak and cation cycling, but also on proton slip
 192 within the proton pumps and the structural integrity of the mitochondria. A more
 193 loosely coupled state is induced by stimulation of mitochondrial superoxide
 194 formation and the bypass of proton pumps. In addition, uncoupling by application
 195 of protonophores represents an experimental intervention for the transition from a
 196 well-coupled to the noncoupled state of mitochondrial respiration.
- 197 6. Respiratory oxygen consumption rates have to be carefully normalized to enable meta-
 198 analytic studies beyond the specific question of a particular experiment. Therefore,
 199 all raw data should be published in a supplemental table or open access data
 200 repository. Normalization of rates for the volume of the experimental chamber (the
 201 measuring system) is distinguished from normalization for (1) the volume or mass
 202 of the experimental sample, (2) the number of objects (cells, organisms), and (3)
 203 the concentration of mitochondrial markers in the chamber.
- 204 7. The consistent use of terms and symbols discussed in this MitoEAGLE position
 205 statement will facilitate transdisciplinary communication and support further
 206 developments of a database on bioenergetics and mitochondrial physiology. The
 207 present considerations are focused on studies with mitochondrial preparations.
 208 These will be extended in a series of reports on pathway control of mitochondrial
 209 respiration, the protonmotive force, respiratory states in intact cells, and
 210 harmonization of experimental procedures.

215 **Box 1: In brief – Mitochondria and Bioblasts**

216 **Mitochondria** are the oxygen-consuming electrochemical generators evolved from
 217 endosymbiotic bacteria (Margulis 1970; Lane 2005). They were described by Richard Altmann
 218 (1894) as ‘bioblasts’, which include not only the mitochondria as presently defined, but also
 219 symbiotic and free-living bacteria. The word ‘mitochondria’ (Greek mitos: thread; chondros:
 220 granule) was introduced by Carl Benda (1898).

221 We now recognize mitochondria as dynamic organelles with a double membrane that are
 222 contained within eukaryotic cells. The mitochondrial inner membrane (mtIM) shows dynamic
 223 tubular to disk-shaped cristae that separate the mitochondrial matrix, *i.e.*, the negatively charged
 224 internal mitochondrial compartment, and the intermembrane space; the latter being positively
 225 charged and enclosed by the mitochondrial outer membrane (mtOM). The mtIM contains the
 226 non-bilayer phospholipid cardiolipin, which is not present in any other eukaryotic cellular
 227 membrane. Cardiolipin promotes the formation of respiratory supercomplexes (SC I_nIII_nIV_n),
 228 which are supramolecular assemblies based upon specific, though dynamic, interactions
 229 between individual respiratory complexes (Greggio *et al.* 2017; Lenaz *et al.* 2017). Membrane
 230

231 fluidity exerts an influence on functional properties of proteins incorporated in the membranes
 232 (Waczulikova *et al.* 2007).

233 Mitochondria are the structural and functional elements of cell respiration. Cell
 234 respiration is the reduction of oxygen by electron transfer coupled to electrochemical proton
 235 translocation across the mtIM. In the process of oxidative phosphorylation (OXPHOS), the
 236 catabolic reaction of oxygen consumption is electrochemically coupled to the transformation of
 237 energy in the form of adenosine triphosphate (ATP; Mitchell 1961, 2011). Mitochondria are the
 238 powerhouses of the cell which contain the machinery of the OXPHOS-pathways, including
 239 transmembrane respiratory complexes—proton pumps with FMN, Fe-S and cytochrome *b, c,*
 240 *aa₃* redox systems); alternative dehydrogenases and oxidases; the coenzyme ubiquinone (Q);
 241 F-ATPase or ATP synthase; the enzymes of the tricarboxylic acid cycle and fatty acid oxidation;
 242 transporters of ions, metabolites and co-factors; and mitochondrial kinases related to energy
 243 transfer pathways. The mitochondrial proteome comprises over 1,200 proteins (Calvo *et al.*
 244 2015; 2017), mostly encoded by nuclear DNA (nDNA), with a variety of functions, many of
 245 which are relatively well known (*e.g.*, apoptosis-regulating proteins), while others are still under
 246 investigation, or need to be identified (*e.g.*, alanine transporter).

247 There is a constant crosstalk between mitochondria and the other cellular components.
 248 The crosstalk between mitochondria and endoplasmic reticulum is involved in the regulation of
 249 calcium homeostasis, cell division, autophagy, differentiation, anti-viral signaling (Murley and
 250 Nunnari 2016). Cellular mitostasis is maintained through regulation at both the transcriptional
 251 and post-translational level, through cell signalling including proteostatic (*e.g.*, the ubiquitin-
 252 proteasome and autophagy-lysosome pathways), and genome stability modules throughout the
 253 cell cycle or even cell death, contributing to homeostatic regulation in response to varying
 254 energy demands and stress (Quiros *et al.* 2016). In addition to mitochondrial movement along
 255 microtubules, mitochondrial morphology can change in response to energy requirements of the
 256 cell via processes known as fusion and fission, through which mitochondria communicate
 257 within a network, and in response to intracellular stress factors causing swelling and ultimately
 258 permeability transition.

259 Mitochondria typically maintain several copies of their own genome known as
 260 mitochondrial DNA (mtDNA; hundred to thousands per cell; Cummins 1998), which is
 261 maternally inherited. One exception to strictly maternal inheritance in animals is found in
 262 bivalves (Breton *et al.* 2007; White *et al.* 2008). mtDNA is compact (16.5 kB in humans) and
 263 encodes 13 protein subunits of the transmembrane respiratory Complexes CI, CIII, CIV and F-
 264 ATPase, 22 tRNAs, and two RNAs. Additional gene content has been suggested to include
 265 microRNAs, piRNA, smithRNAs, repeat associated RNA, and even additional proteins (Duarte
 266 *et al.* 2014; Lee *et al.* 2015; Cobb *et al.* 2016). The mitochondrial genome requires nuclear-
 267 encoded mitochondrial targeted proteins for its maintenance and expression (Rackham *et al.*
 268 2012).

269 Abbreviation: mt, as generally used in mtDNA. Mitochondrion is singular and
 270 mitochondria is plural.

271 *‘For the physiologist, mitochondria afforded the first opportunity for an experimental*
 272 *approach to structure-function relationships, in particular those involved in active transport,*
 273 *vectorial metabolism, and metabolic control mechanisms on a subcellular level’* (Ernster and
 274 Schatz 1981).

275

276 1. Introduction

277

278 Mitochondria are the powerhouses of the cell with numerous physiological, molecular,
 279 and genetic functions (**Box 1**). Every study of mitochondrial health and disease is faced with
 280 **E**volution, **A**ge, **G**ender and sex, **L**ifestyle, and **E**nvironment (EAGLE) as essential background
 281 conditions intrinsic to the individual patient or subject, cohort, species, tissue and to some extent

282 even cell line. As a large and coordinated group of laboratories and researchers, the mission of
283 the global MitoEAGLE Network is to generate the necessary scale, type, and quality of
284 consistent data sets and conditions to address this intrinsic complexity. Harmonization of
285 experimental protocols and implementation of a quality control and data management system
286 are required to interrelate results gathered across a spectrum of studies and to generate a
287 rigorously monitored database focused on mitochondrial respiratory function. In this way,
288 researchers within the same and across different disciplines will be positioned to compare
289 findings across traditions and generations to an agreed upon set of clearly defined and accepted
290 international standards.

291 Reliability and comparability of quantitative results depend on the accuracy of
292 measurements under strictly-defined conditions. A conceptual framework is required to warrant
293 meaningful interpretation and comparability of experimental outcomes carried out by research
294 groups at different institutes. With an emphasis on quality of research, collected data can be
295 useful far beyond the specific question of a particular experiment. Enabling meta-analytic
296 studies is the most economic way of providing robust answers to biological questions (Cooper
297 *et al.* 2009). Vague or ambiguous jargon can lead to confusion and may relegate valuable
298 signals to wasteful noise. For this reason, measured values must be expressed in standard units
299 for each parameter used to define mitochondrial respiratory function. Harmonization of
300 nomenclature and definition of technical terms are essential to improve the awareness of the
301 intricate meaning of current and past scientific vocabulary, for documentation and integration
302 into databases in general, and quantitative modelling in particular (Beard 2005). The focus on
303 coupling states and fluxes through metabolic pathways of aerobic energy transformation in
304 mitochondrial preparations is a first step in the attempt to generate a conceptually-oriented
305 nomenclature in bioenergetics and mitochondrial physiology. Coupling states of intact cells,
306 the protonmotive force, and respiratory control by fuel substrates and specific inhibitors of
307 respiratory enzymes will be reviewed in subsequent communications.

308
309

310 **2. Oxidative phosphorylation and coupling states in mitochondrial preparations**

311 *‘Every professional group develops its own technical jargon for talking about matters of*
312 *critical concern ... People who know a word can share that idea with other members of*
313 *their group, and a shared vocabulary is part of the glue that holds people together and*
314 *allows them to create a shared culture’ (Miller 1991).*

315

316 **Mitochondrial preparations** are defined as either isolated mitochondria, or tissue and
317 cellular preparations in which the barrier function of the plasma membrane is disrupted. Since
318 this entails the loss of cell viability, mitochondrial preparations are not studied *in vivo*. In
319 contrast to isolated mitochondria and tissue homogenate preparations, mitochondria in
320 permeabilized tissues and cells are *in situ* relative to the plasma membrane. The plasma
321 membrane separates the intracellular compartment including the cytosol, nucleus, and
322 organelles from the environment of the cell. The plasma membrane consists of a lipid bilayer,
323 embedded proteins, and attached organic molecules that collectively control the selective
324 permeability of ions, organic molecules, and particles across the cell boundary. The intact
325 plasma membrane prevents the passage of many water-soluble mitochondrial substrates and
326 inorganic ions—such as succinate, adenosine diphosphate (ADP) and inorganic phosphate (P_i),
327 that must be controlled at kinetically-saturating concentrations for the analysis of respiratory
328 capacities; this limits the scope of investigations into mitochondrial respiratory function in
329 intact cells.

330 The cholesterol content of the plasma membrane is high compared to mitochondrial
331 membranes. Therefore, mild detergents—such as digitonin and saponin—can be applied to
332 selectively permeabilize the plasma membrane by interaction with cholesterol and allow free

333 exchange of organic molecules and inorganic ions between the cytosol and the immediate cell
 334 environment, while maintaining the integrity and localization of organelles, cytoskeleton, and
 335 the nucleus. Application of optimum concentrations of permeabilization agents (mild detergents
 336 or toxins) leads to washout of cytosolic marker enzymes—such as lactate dehydrogenase—and
 337 results in the complete loss of cell viability, tested by nuclear staining using membrane-
 338 impermeable dyes, while mitochondrial function remains intact. Respiration of isolated
 339 mitochondria remains unaltered after the addition of low concentrations of digitonin or saponin.
 340 In addition to mechanical permeabilization during homogenization of tissue, permeabilization
 341 agents may be applied to ensure permeabilization of all cells. Suspensions of cells
 342 permeabilized in the respiration chamber and crude tissue homogenates contain all components
 343 of the cell at highly dilute concentrations. All mitochondria are retained in chemically-
 344 permeabilized mitochondrial preparations and crude tissue homogenates. In the preparation of
 345 isolated mitochondria, the cells or tissues are homogenized, and the mitochondria are separated
 346 from other cell fractions and purified by differential centrifugation, entailing the loss of a
 347 fraction of the total mitochondrial content. Typical mitochondrial recovery ranges from 30% to
 348 80%. Maximization of the purity of isolated mitochondria may compromise not only the
 349 mitochondrial yield but also the structural and functional integrity. Therefore, protocols to
 350 isolate mitochondria need to be optimized according to each study. The term mitochondrial
 351 preparation does not include further fractionation of mitochondrial components, neither
 352 submitochondrial particles.

353

354 2.1. Respiratory control and coupling

355

356 Respiratory coupling control states are established in studies of mitochondrial
 357 preparations to obtain reference values for various output variables. Physiological conditions *in*
 358 *vivo* deviate from these experimentally obtained states. Since kinetically-saturating
 359 concentrations, *e.g.*, of ADP or oxygen (O₂; dioxygen), may not apply to physiological
 360 intracellular conditions, relevant information is obtained in studies of kinetic responses to
 361 variations in [ADP] or [O₂] in the range between kinetically-saturating concentrations and
 362 anoxia (Gnaiger 2001).

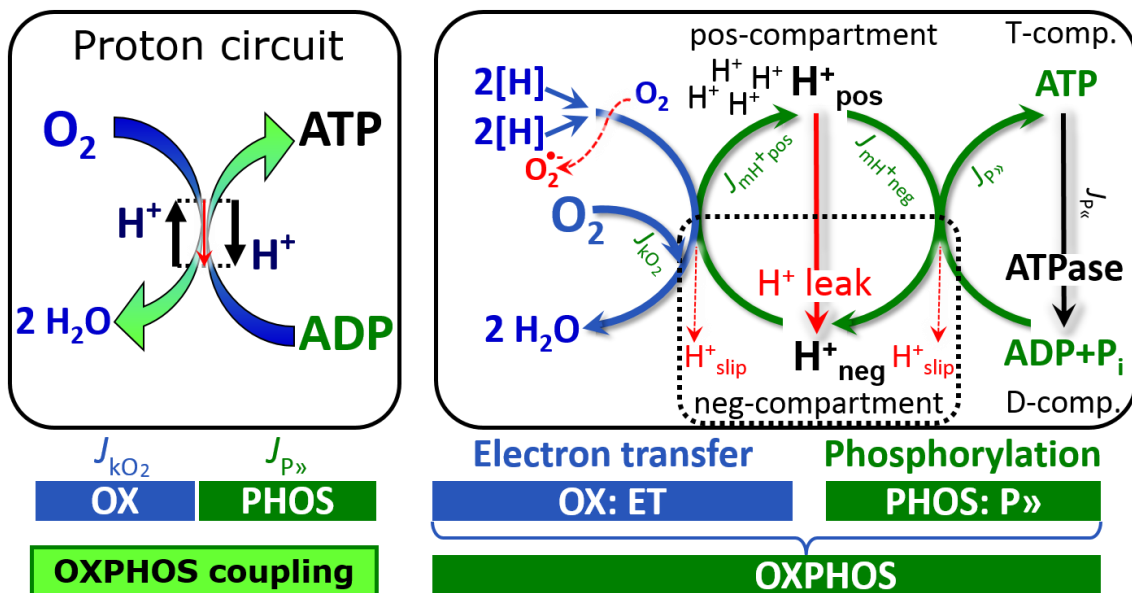
363

364 **The steady-state:** Mitochondria represent a thermodynamically open system in non-
 365 equilibrium states of biochemical energy transformation. State variables (protonmotive force;
 366 redox states) and metabolic *rates* (fluxes) are measured in defined mitochondrial respiratory
 367 *states*. Steady-states can be obtained only in open systems, in which changes by *internal*
 368 transformations, *e.g.*, O₂ consumption, are instantaneously compensated for by *external* fluxes,
 369 *e.g.*, O₂ supply, preventing a change of O₂ concentration in the system (Gnaiger 1993b).
 370 Mitochondrial respiratory states monitored in closed systems satisfy the criteria of pseudo-
 371 steady states for limited periods of time, when changes in the system (concentrations of O₂, fuel
 372 substrates, ADP, P_i, H⁺) do not exert significant effects on metabolic fluxes (respiration,
 373 phosphorylation). Such pseudo-steady states require respiratory media with sufficient buffering
 374 capacity and substrates maintained at kinetically-saturating concentrations, and thus depend on
 the kinetics of the processes under investigation.

375

376 **Specification of biochemical dose:** Substrates, uncouplers, inhibitors, and other
 377 biochemical reagents are titrated to dissect mitochondrial function. Nominal concentrations of
 378 these substances are usually reported as initial amount of substance concentration [mol·L⁻¹] in
 379 the incubation medium. When aiming at the measurement of kinetically saturated processes—
 380 such as OXPHOS-capacities, the concentrations for substrates can be chosen according to the
 381 apparent equilibrium constant, K_m' . In the case of hyperbolic kinetics, only 80% of maximum
 382 respiratory capacity is obtained at a substrate concentration of four times the K_m' , whereas
 383 substrate concentrations of 5, 9, 19 and 49 times the K_m' are theoretically required for reaching
 83%, 90%, 95% or 98% of the maximal rate (Gnaiger 2001). Other reagents are chosen to

384 inhibit or alter some processes. The amount of these chemicals in an experimental incubation
 385 is selected to maximize effect, avoiding unacceptable off-target consequences that would
 386 adversely affect the data being sought. Specifying the amount of substance in an incubation as
 387 nominal concentration in the aqueous incubation medium can be ambiguous (Doskey *et al.*
 388 2015), particularly for lipophilic substances (oligomycin; uncouplers, permeabilization agents)
 389 or cations (TPP⁺; fluorescent dyes such as safranin, TMRM), which accumulate in biological
 390 membranes or in the mitochondrial matrix. For example, a dose of digitonin of 8 fmol·cell⁻¹ (10
 391 pg·cell⁻¹; 10 μg·10⁻⁶ cells) is optimal for permeabilization of endothelial cells, and the
 392 concentration in the incubation medium has to be adjusted according to the cell density applied
 393 (Doerrier *et al.* 2018). Generally, dose/exposure can be specified per unit of biological sample,
 394 *i.e.*, (nominal moles of xenobiotic)/(number of cells) [mol·cell⁻¹] or, as appropriate, per mass of
 395 biological sample [mol·kg⁻¹]. This approach to specification of dose/exposure provides a
 396 scalable parameter that can be used to design experiments, help interpret a wide variety of
 397 experimental results, and provide absolute information that allows researchers worldwide to
 398 make the most use of published data (Doskey *et al.* 2015).
 399



400
 401 **Fig. 2. The proton circuit and coupling in oxidative phosphorylation (OXPHOS).** 2[H]
 402 indicates the reduced hydrogen equivalents of fuel substrates of the catabolic reaction *k* with
 403 oxygen. O₂ flux, *J*_{kO₂}, through the catabolic ET-pathway, is coupled to flux through the
 404 phosphorylation-pathway of ADP to ATP, *J*_{P»}. The proton pumps of the ET-pathway drive
 405 proton flux into the positive (pos) compartment, *J*_{mH⁺pos}, generating the output protonmotive
 406 force (motive, subscript *m*). F-ATPase is coupled to inward proton current into the negative
 407 (neg) compartment, *J*_{mH⁺neg}, to phosphorylate ADP+P_i to ATP. The system defined by the
 408 boundaries (full black line) is not a black box, but is analysed as a compartmental system. The
 409 negative compartment (neg-compartment, enclosed by the dotted line) is the matrix space,
 410 separated by the mtIM from the positive compartment (pos-compartment). ADP+P_i and ATP
 411 are the substrate- and product-compartments (scalar ADP and ATP compartments, D-comp.
 412 and T-comp.), respectively. At steady-state proton turnover, *J*_{∞H⁺}, and ATP turnover, *J*_{∞P},
 413 maintain concentrations constant, when *J*<sub>mH⁺∞} = *J*<sub>mH⁺pos} = *J*<sub>mH⁺neg}, and *J*<sub>P∞} = *J*<sub>P»} = *J*<sub>P«}. Modified
 414 from Gnaiger (2014).
 415</sub></sub></sub></sub></sub></sub>

416 **Phosphorylation, P», and P»/O₂ ratio:** *Phosphorylation* in the context of OXPHOS is
 417 defined as phosphorylation of ADP by P_i to ATP. On the other hand, the term phosphorylation
 418 is used generally in many contexts, *e.g.*, protein phosphorylation. This justifies consideration

419 of a symbol more discriminating and specific than P as used in the P/O ratio (phosphate to
 420 atomic oxygen ratio), where P indicates phosphorylation of ADP to ATP or GDP to GTP. We
 421 propose the symbol P» for the endergonic (uphill) direction of phosphorylation ADP→ATP,
 422 and likewise the symbol P« for the corresponding exergonic (downhill) hydrolysis ATP→ADP
 423 (Fig. 2). P» refers mainly to electrontransfer phosphorylation but may also involve substrate-
 424 level phosphorylation as part of the tricarboxylic acid (TCA) cycle (succinyl-CoA ligase;
 425 phosphoglycerate kinase) and phosphorylation of ADP catalyzed by pyruvate kinase, and of
 426 GDP phosphorylated by phosphoenolpyruvate carboxykinase. Transphosphorylation is
 427 performed by adenylate kinase, creatine kinase, hexokinase and nucleoside diphosphate kinase.
 428 In isolated mammalian mitochondria, ATP production catalyzed by adenylate kinase (2 ADP
 429 ↔ ATP + AMP) proceeds without fuel substrates in the presence of ADP (Komlódi and Tretter
 430 2017). Kinase cycles are involved in intracellular energy transfer and signal transduction for
 431 regulation of energy flux.

432 The P»/O₂ ratio (P»/4 e⁻) is two times the ‘P/O’ ratio (P»/2 e⁻) of classical bioenergetics.
 433 P»/O₂ is a generalized symbol, independent phosphorylation assessment by determination of P_i
 434 consumption (P_i/O₂ flux ratio), ADP depletion (ADP/O₂ flux ratio), or ATP production
 435 (ATP/O₂ flux ratio). The mechanistic P»/O₂ ratio—or P»/O₂ stoichiometry—is calculated from
 436 the proton-to-O₂ and proton-to-phosphorylation coupling stoichiometries (Fig. 1A),
 437

$$438 \quad P\gg/O_2 = \frac{H_{\text{pos}}^+/O_2}{H_{\text{neg}}^+/P\gg} \quad (1)$$

439
 440 The H⁺_{pos}/O₂ coupling stoichiometry (referring to the full 4 electron reduction of O₂) depends
 441 on the ET-pathway control state which defines the relative involvement of the three coupling
 442 sites (CI, CIII and CIV) in the catabolic pathway of electrons to O₂. This varies with: (1) a
 443 bypass of CI by single or multiple electron input into the Q-junction; and (2) a bypass of CIV
 444 by involvement of AOX. H⁺_{pos}/O₂ is 12 in the ET-pathways involving CIII and CIV as proton
 445 pumps, increasing to 20 for the NADH-pathway (Fig. 1A), but a general consensus on H⁺_{pos}/O₂
 446 stoichiometries remains to be reached (Hinkle 2005; Wikström and Hummer 2012; Sazanov
 447 2015). The H⁺_{neg}/P» coupling stoichiometry (3.7; Fig. 1A) is the sum of 2.7 H⁺_{neg} required by
 448 the F-ATPase of vertebrate and most invertebrate species (Watt *et al.* 2010) and the proton
 449 balance in the translocation of ADP, ATP and P_i (Fig. 1B). Taken together, the mechanistic
 450 P»/O₂ ratio is calculated at 5.4 and 3.3 for NADH- and succinate-linked respiration, respectively
 451 (Eq. 1). The corresponding classical P»/O ratios (referring to the 2 electron reduction of 0.5 O₂)
 452 are 2.7 and 1.6 (Watt *et al.* 2010), in agreement with the measured P»/O ratio for succinate of
 453 1.58 ± 0.02 (Gnaiger *et al.* 2000).

454 The effective P»/O₂ flux ratio (Y_{P»/O₂} = J_{P»}/J_{KO₂}) is diminished relative to the mechanistic
 455 P»/O₂ ratio by intrinsic and extrinsic uncoupling and dyscoupling (Fig. 3). Such generalized
 456 uncoupling is different from switching to mitochondrial pathways that involve fewer than three
 457 proton pumps (‘coupling sites’: Complexes CI, CIII and CIV), bypassing CI through multiple
 458 electron entries into the Q-junction, or CIII and CIV through AOX (Fig. 1). Reprogramming of
 459 mitochondrial pathways may be considered as a switch of gears (changing the stoichiometry)
 460 rather than uncoupling (loosening the stoichiometry). In addition, Y_{P»/O₂} depends on several
 461 experimental conditions of flux control, increasing as a hyperbolic function of [ADP] to a
 462 maximum value (Gnaiger 2001).

463 **Control and regulation:** The terms metabolic *control* and *regulation* are frequently used
 464 synonymously, but are distinguished in metabolic control analysis: ‘We could understand the
 465 regulation as the mechanism that occurs when a system maintains some variable constant over
 466 time, in spite of fluctuations in external conditions (homeostasis of the internal state). On the
 467 other hand, metabolic control is the power to change the state of the metabolism in response to
 468 an external signal’ (Fell 1997). Respiratory control may be induced by experimental control

469 signals that *exert* an influence on: (1) ATP demand and ADP phosphorylation-rate; (2) fuel
 470 substrate composition, pathway competition; (3) available amounts of substrates and O₂, *e.g.*,
 471 starvation and hypoxia; (4) the protonmotive force, redox states, flux–force relationships,
 472 coupling and efficiency; (5) Ca²⁺ and other ions including H⁺; (6) inhibitors, *e.g.*, nitric oxide
 473 or intermediary metabolites such as oxaloacetate; (7) signalling pathways and regulatory
 474 proteins, *e.g.*, insulin resistance, transcription factor hypoxia inducible factor 1. *Mechanisms* of
 475 respiratory control and regulation include adjustments of: (1) enzyme activities by allosteric
 476 mechanisms and phosphorylation; (2) enzyme content, concentrations of cofactors and
 477 conserved moieties—such as adenylates, nicotinamide adenine dinucleotide [NAD⁺/NADH],
 478 coenzyme Q, cytochrome *c*); (3) metabolic channeling by supercomplexes; and (4)
 479 mitochondrial density (enzyme concentrations and membrane area) and morphology (cristae
 480 folding, fission and fusion). Mitochondria are targeted directly by hormones, thereby affecting
 481 their energy metabolism (Lee *et al.* 2013; Gerö and Szabo 2016; Price and Dai 2016; Moreno
 482 *et al.* 2017). Evolutionary or acquired differences in the genetic and epigenetic basis of
 483 mitochondrial function (or dysfunction) between subjects and gene therapy; age; gender,
 484 biological sex, and hormone concentrations; life style including exercise and nutrition; and
 485 environmental issues including thermal, atmospheric, toxicological and pharmacological
 486 factors, exert an influence on all control mechanisms listed above. For reviews, see Brown
 487 1992; Gnaiger 1993a, 2009; 2014; Paradies *et al.* 2014; Morrow *et al.* 2017.

488 **Respiratory control and response:** Lack of control by a metabolic pathway, *e.g.*,
 489 phosphorylation-pathway, means that there will be no response to a variable activating it, *e.g.*,
 490 [ADP]. The reverse, however, is not true as the absence of a response to [ADP] does not exclude
 491 the phosphorylation-pathway from having some degree of control. The degree of control of a
 492 component of the OXPHOS-pathway on an output variable—such as O₂ flux, will in general
 493 be different from the degree of control on other outputs—such as phosphorylation-flux or
 494 proton leak flux. Therefore, it is necessary to be specific as to which input and output are under
 495 consideration (Fell 1997).

496 **Respiratory coupling control and ET-pathway control:** Respiratory control refers to
 497 the ability of mitochondria to adjust O₂ flux in response to external control signals by engaging
 498 various mechanisms of control and regulation. Respiratory control is monitored in a
 499 mitochondrial preparation under conditions defined as respiratory states. When
 500 phosphorylation of ADP to ATP is stimulated or depressed, an increase or decrease is observed
 501 in electron flux linked to O₂ flux in respiratory coupling states of intact mitochondria
 502 (‘controlled states’ in the classical terminology of bioenergetics). Alternatively, coupling of
 503 electron transfer with phosphorylation is disengaged by disruption of the integrity of the mtIM
 504 or by uncouplers, functioning like a clutch in a mechanical system. The corresponding coupling
 505 control state is characterized by high levels of O₂ consumption without control by P»
 506 (‘uncontrolled state’).

507 ET-pathway control states are obtained in mitochondrial preparations by depletion of
 508 endogenous substrates and addition to the mitochondrial respiration medium of fuel substrates
 509 (CHNO; 2[H] in **Fig. 2**) and specific inhibitors, activating selected mitochondrial catabolic
 510 pathways, *k* (**Fig. 1**). Coupling control states and pathway control states are complementary,
 511 since mitochondrial preparations depend on an exogenous supply of pathway-specific fuel
 512 substrates and oxygen (Gnaiger 2014).

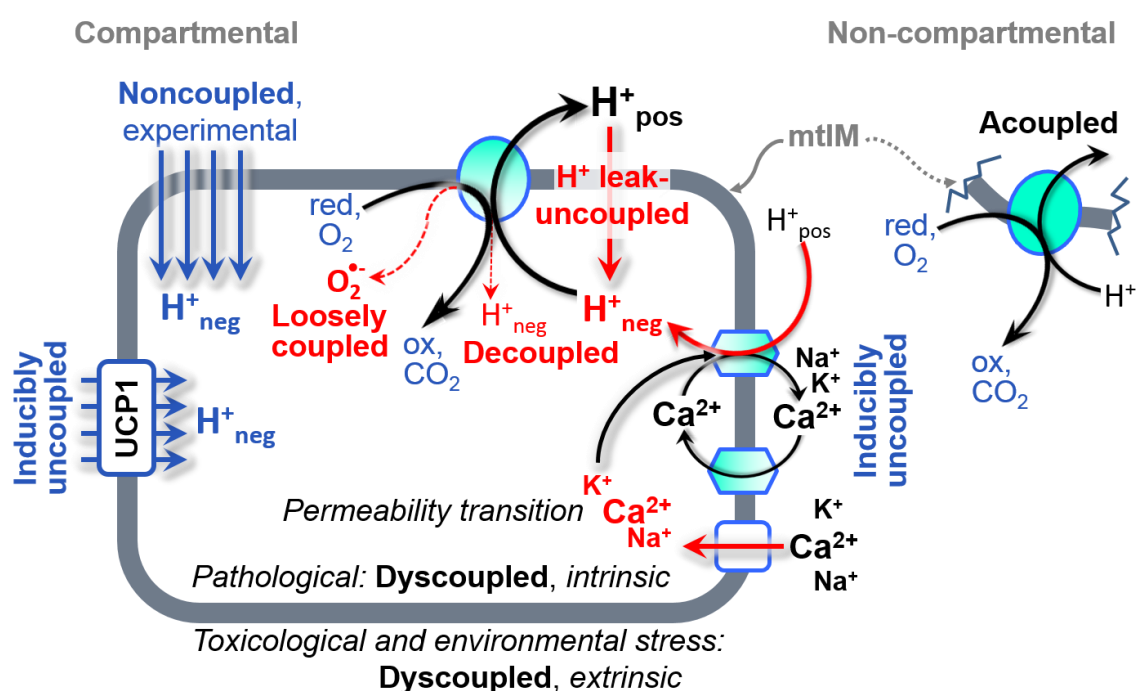
513 **Coupling:** In mitochondrial electron transfer (**Fig. 1**), vectorial transmembrane proton
 514 flux is coupled through the proton pumps CI, CIII and CIV to the catabolic flux of scalar
 515 reactions, collectively measured as O₂ flux (**Fig. 2**). Thus mitochondria are elements of energy
 516 transformation. Energy cannot be lost or produced in any internal process (First Law of
 517 thermodynamics). Open and closed systems can gain or lose energy only by external fluxes—
 518 by exchange with the environment. Energy is a conserved quantity. Therefore, energy can
 519 neither be produced by mitochondria, nor is there any internal process without energy

520 conservation. Exergy is defined as the ‘free energy’ with the potential to perform work.
 521 *Coupling* is the mechanistic linkage of an exergonic process (spontaneous, negative exergy
 522 change) with an endergonic process (positive exergy change) in energy transformations which
 523 conserve part of the exergy that would be irreversible lost or dissipated in an uncoupled process.

524 **Uncoupling:** Uncoupling of mitochondrial respiration is a general term comprising
 525 diverse mechanisms. Differences of terms—uncoupled vs. noncoupled—are easily overlooked,
 526 although they relate to different mechanisms of uncoupling (**Fig. 3**).

- 527 1. Proton leak across the mtIM from the pos- to the neg-compartment (**Fig. 2**);
- 528 2. Cycling of other cations, strongly stimulated by permeability transition;
- 529 3. Proton slip in the proton pumps when protons are effectively not pumped (CI, CIII and
 530 CIV) or are not driving phosphorylation (F-ATPase);
- 531 4. Loss of compartmental integrity when electron transfer is uncoupled;
- 532 5. Electron leak in the loosely coupled univalent reduction of O_2 to superoxide ($O_2^{\cdot-}$;
 533 superoxide anion radical).

534



535

536 **Fig 3. Mechanisms of respiratory uncoupling.** An intact mitochondrial inner membrane,
 537 mtIM, is required for vectorial, compartmental coupling. ‘Acoupled’ respiration is the
 538 consequence of structural disruption with catalytic activity of non-compartmental
 539 mitochondrial fragments. Inducibly uncoupled (activation of UCP1) and experimentally
 540 noncoupled respiration (titration of protonophores) stimulate respiration to maximum O_2 flux.
 541 H^+ leak-uncoupled, decoupled, and loosely coupled respiration are components of intrinsic
 542 uncoupling. Pathological dysfunction may affect all types of uncoupling, including
 543 permeability transition, causing intrinsically dyscoupled respiration. Similarly, toxicological
 544 and environmental stress factors can cause extrinsically dyscoupled respiration.

545

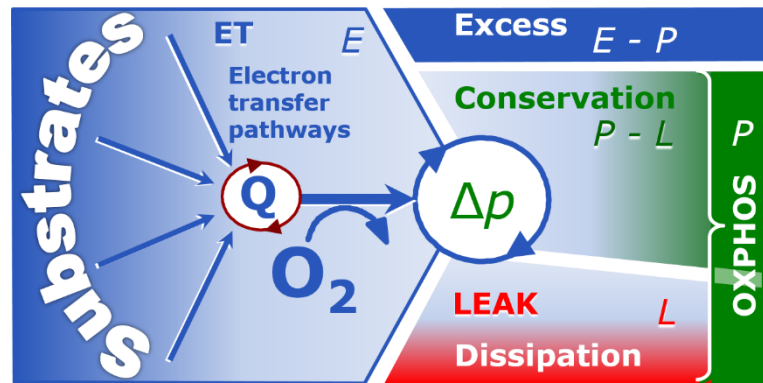
546 2.2. Coupling states and respiratory rates

547

548 **Respiratory capacities in coupling control states:** To extend the classical nomenclature
 549 on mitochondrial coupling states (Section 2.3) by a concept-driven terminology that
 550 incorporates explicitly information on the nature of respiratory states, the terminology must be
 551 general and not restricted to any particular experimental protocol or mitochondrial preparation
 552 (Gnaiger 2009). We focus primarily on the conceptual ‘why’, along with clarification of the

553 experimental ‘how’. Respiratory capacities delineate, comparable to channel capacity in
 554 information theory (Schneider 2006), the upper bound of the rate of respiration measured in
 555 defined coupling control states and electron transfer-pathway (ET-pathway) states (**Fig. 4**).
 556

557 **Fig. 4. Four-compartment**
 558 **model of oxidative**
 559 **phosphorylation.** Respiratory
 560 states (ET, OXPHOS, LEAK;
 561 **Table 1**) and corresponding rates
 562 (E , P , L) are connected by the
 563 protonmotive force, Δp . ET-
 564 capacity, E , is partitioned into (1)
 565 dissipative LEAK-respiration, L ,
 566 when the Gibbs energy change of
 567 catabolic O_2 flux is irreversibly
 568 lost, (2) net OXPHOS-capacity, $P-L$,
 569 and (3) the excess capacity, $E-P$. Modified from Gnaiger (2014).
 570



571 **Table 1. Coupling states and residual oxygen consumption in mitochondrial**
 572 **preparations in relation to respiration- and phosphorylation-flux, J_{kO_2} and $J_{P_{\gg}}$,**
 573 **and protonmotive force, Δp .** Coupling states are established at kinetically-saturating
 574 concentrations of fuel substrates and O_2 .

State	J_{kO_2}	$J_{P_{\gg}}$	Δp	Inducing factors	Limiting factors
LEAK	L ; low, cation leak-dependent respiration	0	max.	proton leak, slip, and cation cycling	$J_{P_{\gg}} = 0$: (1) without ADP, L_N ; (2) max. ATP/ADP ratio, L_T ; or (3) inhibition of the phosphorylation-pathway, L_{Omy}
OXPHOS	P ; high, ADP-stimulated respiration	max.	high	kinetically-saturating [ADP] and $[P_i]$	$J_{P_{\gg}}$ by phosphorylation-pathway; or J_{kO_2} by ET-capacity
ET	E ; max., noncoupled respiration	0	low	optimal external uncoupler concentration for max. $J_{O_2,E}$	J_{kO_2} by ET-capacity
ROX	R_{ox} ; min., residual O_2 consumption	0	0	$J_{O_2,Rox}$ in non-ET-pathway oxidation reactions	full inhibition of ET-pathway; or absence of fuel substrates

575
 576 To provide a diagnostic reference for respiratory capacities of core energy metabolism,
 577 the capacity of *oxidative phosphorylation*, OXPHOS, is measured at kinetically-saturating
 578 concentrations of ADP and P_i . The *oxidative* ET-capacity reveals the limitation of OXPHOS-
 579 capacity mediated by the *phosphorylation*-pathway. The ET- and phosphorylation-pathways
 580 comprise coupled segments of the OXPHOS-system. ET-capacity is measured as noncoupled
 581 respiration by application of *external uncouplers*. The contribution of *intrinsically uncoupled*
 582 O_2 consumption is studied in the absence of ADP—by not stimulating phosphorylation, or by
 583 inhibition of the phosphorylation-pathway. The corresponding states are collectively classified

584 as LEAK-states, when O₂ consumption compensates mainly for ion leaks, including the proton
 585 leak. Defined coupling states are induced by: (1) adding cation chelators such as EGTA, binding
 586 free Ca²⁺ and thus limiting cation cycling; (2) adding ADP and P_i; (3) inhibiting the
 587 phosphorylation-pathway; and (4) uncoupler titrations, while maintaining a defined ET-
 588 pathway state with constant fuel substrates and inhibitors of specific branches of the ET-
 589 pathway (**Fig. 1**).

590 The three coupling states, ET, LEAK and OXPHOS, are shown schematically with the
 591 corresponding respiratory rates, abbreviated as *E*, *L* and *P*, respectively (**Fig. 4**). We distinguish
 592 metabolic *pathways* from metabolic *states* and the corresponding metabolic *rates*; for example:
 593 ET-pathways (**Fig. 4**), ET-state (**Fig. 5C**), and ET-capacity, *E*, respectively (**Table 1**). The
 594 protonmotive force is *high* in the OXPHOS-state when it drives phosphorylation, *maximum* in
 595 the LEAK-state of coupled mitochondria, driven by LEAK-respiration at a minimum back flux
 596 of cations to the matrix side, and *very low* in the ET-state when uncouplers short-circuit the
 597 proton cycle (**Table 1**).

598 *E* may exceed or be equal to *P*. *E* > *P* is observed in many types of mitochondria, varying
 599 between species, tissues and cell types (Gnaiger 2009). *E*-*P* is the excess ET-capacity pushing
 600 the phosphorylation-flux (**Fig. 1B**) to the limit of its *capacity of utilizing* the protonmotive force.
 601 In addition, the magnitude of *E*-*P* depends on the tightness of respiratory coupling or degree of
 602 uncoupling, since an increase of *L* causes *P* to increase towards the limit of *E*. The *excess E*-*P*
 603 capacity, *E*-*P*, therefore, provides a sensitive diagnostic indicator of specific injuries of the
 604 phosphorylation-pathway, under conditions when *E* remains constant but *P* declines relative to
 605 controls (**Fig. 4**). Substrate cocktails supporting simultaneous convergent electron transfer to
 606 the Q-junction for reconstitution of TCA cycle function establish pathway control states with
 607 high ET-capacity, and consequently increase the sensitivity of the *E*-*P* assay.

608 *E* cannot theoretically be lower than *P*. *E* < *P* must be discounted as an artefact, which
 609 may be caused experimentally by: (1) loss of oxidative capacity during the time course of the
 610 respirometric assay, since *E* is measured subsequently to *P*; (2) using insufficient uncoupler
 611 concentrations; (3) using high uncoupler concentrations which inhibit ET (Gnaiger 2008); (4)
 612 high oligomycin concentrations applied for measurement of *L* before titrations of uncoupler,
 613 when oligomycin exerts an inhibitory effect on *E*. On the other hand, the excess ET-capacity is
 614 overestimated if non-saturating [ADP] or [P_i] are used. See State 3 in the next section.

615 The net OXPHOS-capacity is calculated by subtracting *L* from *P* (**Fig. 4**). Then the net
 616 P_»/O₂ equals P_»/(*P*-*L*), wherein the dissipative LEAK component in the OXPHOS-state may
 617 be overestimated. This can be avoided by measuring LEAK-respiration in a state when the
 618 protonmotive force is adjusted to its slightly lower value in the OXPHOS-state—by titration of
 619 an ET inhibitor (Divakaruni and Brand 2011). Any turnover-dependent components of proton
 620 leak and slip, however, are underestimated under these conditions (Garlid *et al.* 1993). In
 621 general, it is inappropriate to use the term *ATP production* or *ATP turnover* for the difference
 622 of O₂ flux measured in states *P* and *L*. The difference *P*-*L* is the upper limit of the part of
 623 OXPHOS-capacity that is freely available for ATP production (corrected for LEAK-
 624 respiration) and is fully coupled to phosphorylation with a maximum mechanistic stoichiometry
 625 (**Fig. 4**).

626 **LEAK-state (Fig. 5A):** The LEAK-state is defined as a state of mitochondrial respiration
 627 when O₂ flux mainly compensates for ion leaks in the absence of ATP synthesis, at kinetically-
 628 saturating concentrations of O₂ and respiratory fuel substrates. LEAK-respiration is measured
 629 to obtain an estimate of *intrinsic uncoupling* without addition of an experimental uncoupler: (1)
 630 in the absence of adenylates; (2) after depletion of ADP at a maximum ATP/ADP ratio; or (3)
 631 after inhibition of the phosphorylation-pathway by inhibitors of F-ATPase—such as
 632 oligomycin, or of adenine nucleotide translocase—such as carboxyatractyloside. Adjustment
 633 of the nominal concentration of these inhibitors to the density of biological sample applied can
 634 minimize or avoid inhibitory side-effects exerted on ET-capacity or even some dyscoupling.

635 **Proton leak and uncoupled**
 636 **respiration:** Proton leak is a leak
 637 current of protons. The intrinsic proton
 638 leak is the *uncoupled* process in which
 639 protons diffuse across the mtIM in the
 640 dissipative direction of the downhill
 641 protonmotive force without coupling to
 642 phosphorylation (Fig. 5A). The proton
 643 leak flux depends non-linearly on the
 644 protonmotive force (Garlid *et al.* 1989;
 645 Divakaruni and Brand 2011), it is a
 646 property of the mtIM and may be
 647 enhanced due to possible
 648 contaminations by free fatty acids.
 649 Inducible uncoupling mediated by
 650 uncoupling protein 1 (UCP1) is
 651 physiologically controlled, *e.g.*, in
 652 brown adipose tissue. UCP1 is a
 653 member of the mitochondrial carrier
 654 family which is involved in the
 655 translocation of protons across the mtIM
 656 (Klingenberg 2017). Consequently, the
 657 short-circuit diminishes the
 658 protonmotive force and stimulates
 659 electron transfer to O₂ and heat
 660 dissipation without phosphorylation of
 661 ADP.

662 **Cation cycling:** There can
 663 be other cation contributors to
 664 leak current including calcium
 665 and probably magnesium.
 666 Calcium current is balanced by
 667 mitochondrial Na⁺/Ca²⁺
 668 exchange, which is balanced by
 669 Na⁺/H⁺ or K⁺/H⁺ exchanges.
 670 This is another effective
 671 uncoupling mechanism different
 672 from proton leak.

673 **Proton slip and**
 674 **decoupled respiration:** Proton
 675 slip is the *decoupled* process in
 676 which protons are only partially
 677 translocated by a proton pump of
 678 the ET-pathways and slip back
 679 to the original compartment. The
 680 proton leak is the dominant
 681 contributor to the overall leak current in mammalian mitochondria incubated under
 682 physiological conditions at 37 °C, whereas proton slip is increased at lower experimental
 683 temperature (Canton *et al.* 1995). Proton slip can also happen in association with the F-ATPase,
 684 in which the proton slips downhill across the pump to the matrix without contributing to ATP
 685 synthesis. In each case, proton slip is a property of the proton pump and increases with the
 686 pump turnover rate.

687 **Electron leak and loosely coupled respiration:** Superoxide production by the ETS leads
 688 to a bypass of proton pumps and correspondingly lower P_»/O₂ ratio. This depends on the actual
 689 site of electron leak and the scavenging of hydrogen peroxide by cytochrome *c*, whereby
 690 electrons may re-enter the ETS with proton translocation by CIV.

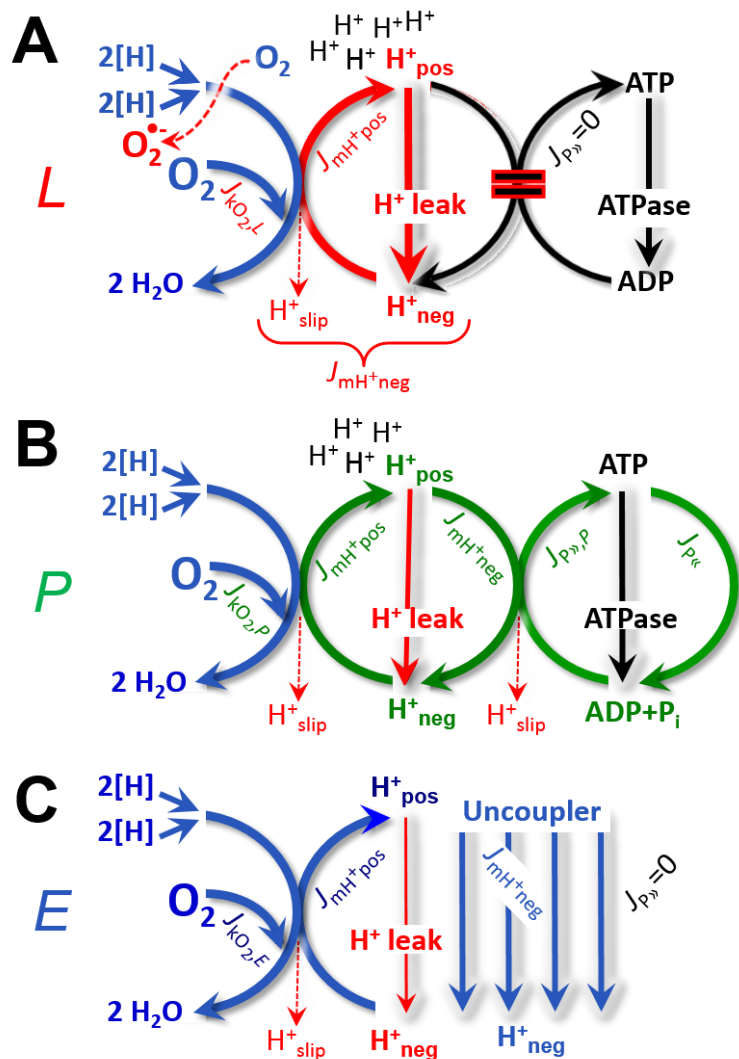


Fig. 5. Respiratory coupling states. A: LEAK-state and rate, L: Phosphorylation is arrested, $J_{P_{\gg}} = 0$, and catabolic O₂ flux, $J_{kO_2,L}$, is controlled mainly by the proton leak, $J_{mH^{+}neg,L}$, at maximum protonmotive force (Fig. 3). **B: OXPHOS-state and rate, P:** Phosphorylation, $J_{P_{\gg}}$, is stimulated by kinetically-saturating [ADP] and [P_i], and is supported by a high protonmotive force. O₂ flux, $J_{kO_2,P}$, is well-coupled at a P_»/O₂ ratio of $J_{P_{\gg},P}/J_{O_2,P}$. **C: ET-state and rate, E:** Noncoupled respiration, $J_{kO_2,E}$, is maximum at optimum exogenous uncoupler concentration and phosphorylation is zero, $J_{P_{\gg}} = 0$. See also Fig. 2.

691 **Table 2. Terms on respiratory coupling and uncoupling.**

Term	J_{kO_2}	$P \gg O_2$	Note	
Acoupled		0	electron transfer in mitochondrial fragments without vectorial proton translocation (Fig. 3)	
intrinsic, no protonophore added	uncoupled	L	0	non-phosphorylating LEAK-respiration (Fig. 5A)
	proton leak-uncoupled		0	component of L , H^+ diffusion across the mtIM (Fig. 3)
	decoupled		0	component of L , proton slip (Fig. 3)
	loosely coupled		0	component of L , lower coupling due to superoxide formation and bypass of proton pumps (Fig. 3)
	dyscoupled		0	pathologically, toxicologically, environmentally increased uncoupling, mitochondrial dysfunction
	inducibly uncoupled		0	by UCP1 or cation (<i>e.g.</i> , Ca^{2+}) cycling (Fig. 3)
noncoupled	E	0	non-phosphorylating respiration stimulated to maximum flux at optimum exogenous uncoupler concentration (Fig. 5C)	
well-coupled	P	high	phosphorylating respiration with an intrinsic LEAK component (Fig. 5B)	
fully coupled	$P - L$	max.	OXPPOS-capacity corrected for LEAK-respiration (Fig. 4)	

692
693 **Loss of compartmental integrity and acoupled respiration:** Electron transfer and
694 catabolic O_2 flux proceed without compartmental proton translocation in disrupted
695 mitochondrial fragments. Such fragments form during mitochondrial isolation, and may not
696 fully fuse to re-establish structurally intact mitochondria. Loss of mtIM integrity, therefore, is
697 the cause of acoupled respiration, which is a nonvectorial dissipative process without control
698 by the protonmotive force.

699 **Dyscoupled respiration:** Mitochondrial injuries may lead to *dyscoupling* as a
700 pathological or toxicological cause of *uncoupled* respiration. Dyscoupling may involve any
701 type of uncoupling mechanism, *e.g.*, opening the permeability transition pore. Dyscoupled
702 respiration is distinguished from the experimentally induced *noncoupled* respiration in the ET-
703 state (**Fig. 3**).

704 **OXPPOS-state (Fig. 5B):** The OXPPOS-state is defined as the respiratory state with
705 kinetically-saturating concentrations of O_2 , respiratory and phosphorylation substrates, and
706 absence of exogenous uncoupler, which provides an estimate of the maximal respiratory
707 capacity in the OXPPOS-state for any given ET-pathway state. Respiratory capacities at
708 kinetically-saturating substrate concentrations provide reference values or upper limits of
709 performance, aiming at the generation of data sets for comparative purposes. Physiological
710 activities and effects of substrate kinetics can be evaluated relative to the OXPPOS-capacity.

711 As discussed previously, 0.2 mM ADP does not fully saturate flux in isolated
712 mitochondria (Gnaiger 2001; Puchowicz *et al.* 2004); greater ADP concentration is required,
713 particularly in permeabilized muscle fibres and cardiomyocytes, to overcome limitations by
714 intracellular diffusion and by the reduced conductance of the mtOM (Jepihhina *et al.* 2011,
715 Illaste *et al.* 2012, Simson *et al.* 2016), either through interaction with tubulin (Rostovtseva *et al.*
716 2008) or other intracellular structures (Birkedal *et al.* 2014). In permeabilized muscle fibre
717 bundles of high respiratory capacity, the apparent K_m for ADP increases up to 0.5 mM (Saks *et*

718 *al.* 1998), consistent with experimental evidence that >90% saturation is reached only at >5
 719 mM ADP (Pesta and Gnaiger 2012). Similar ADP concentrations are also required for accurate
 720 determination of OXPHOS-capacity in human clinical cancer samples and permeabilized cells
 721 (Klepinin *et al.* 2016; Koit *et al.* 2017). Whereas 2.5 to 5 mM ADP is sufficient to obtain the
 722 actual OXPHOS-capacity in many types of permeabilized tissue and cell preparations,
 723 experimental validation is required in each specific case.

724 **Electron transfer-state (Fig. 5C):** The ET-state is defined as the *noncoupled* state with
 725 kinetically-saturating concentrations of O₂, respiratory substrate and optimum *exogenous*
 726 uncoupler concentration for maximum O₂ flux. O₂ flux determined in the ET-state yields an
 727 estimate of ET-capacity. Inhibition of respiration is observed at higher than optimum uncoupler
 728 concentrations. As a consequence of the nearly collapsed protonmotive force, the driving force
 729 is insufficient for phosphorylation, and $J_{P_s} = 0$.

730 **ROX state and *Rox*:** Besides the three fundamental coupling states of mitochondrial
 731 preparations, the state of residual O₂ consumption, ROX, is relevant to assess respiratory
 732 function. ROX is not a coupling state. The rate of residual oxygen consumption, *Rox*, is defined
 733 as O₂ consumption due to oxidative side reactions measured after inhibition of ET—with
 734 rotenone, malonic acid and antimycin A. Cyanide and azide inhibit CIV and several peroxidases
 735 involved in *Rox*. ROX represents a baseline that is used to correct respiration in defined
 736 coupling states. *Rox* is not necessarily equivalent to non-mitochondrial respiration, considering
 737 O₂-consuming reactions in mitochondria not related to ET—such as O₂ consumption in
 738 reactions catalyzed by monoamine oxidases (type A and B), monooxygenases (cytochrome
 739 P450 monooxygenases), dioxygenase (sulfur dioxygenase and trimethyllysine dioxygenase),
 740 and several hydroxylases. Mitochondrial preparations, especially those obtained from liver, may
 741 be contaminated by peroxisomes. This fact makes the exact determination of mitochondrial O₂
 742 consumption and mitochondria-associated generation of reactive oxygen species complicated
 743 (Schönfeld *et al.* 2009). The dependence of ROX-linked O₂ consumption needs to be studied
 744 in detail together with non-ET enzyme activities, availability of specific substrates, O₂
 745 concentration, and electron leakage leading to the formation of reactive oxygen species.

746

747 2.3. Classical terminology for isolated mitochondria

748 *'When a code is familiar enough, it ceases appearing like a code; one forgets that there*
 749 *is a decoding mechanism. The message is identical with its meaning'* (Hofstadter 1979).

750

751 Chance and Williams (1955; 1956) introduced five classical states of mitochondrial respiration
 752 and cytochrome redox states. **Table 3** shows a protocol with isolated mitochondria in a closed
 753 respirometric chamber, defining a sequence of respiratory states. States and rates are not
 754 specifically distinguished in this nomenclature.

755

756

757

758

Table 3. Metabolic states of mitochondria (Chance and Williams, 1956; Table V).

State	[O ₂]	ADP level	Substrate level	Respiration rate	Rate-limiting substance
1	>0	low	low	slow	ADP
2	>0	high	~0	slow	Substrate
3	>0	high	high	fast	respiratory chain
4	>0	low	high	slow	ADP
5	0	high	high	0	Oxygen

759

760 **State 1** is obtained after addition of isolated mitochondria to air-saturated
 761 isoosmotic/isotonic respiration medium containing P_i , but no fuel substrates and no adenylates,
 762 *i.e.*, AMP, ADP, ATP.

763 **State 2** is induced by addition of a ‘high’ concentration of ADP (typically 100 to 300
 764 μM), which stimulates respiration transiently on the basis of endogenous fuel substrates and
 765 phosphorylates only a small portion of the added ADP. State 2 is then obtained at a low
 766 respiratory activity limited by exhausted endogenous fuel substrate availability (**Table 3**). If
 767 addition of specific inhibitors of respiratory complexes—such as rotenone—does not cause a
 768 further decline of O_2 flux, State 2 is equivalent to the ROX state (See below.). If inhibition is
 769 observed, undefined endogenous fuel substrates are a confounding factor of pathway control,
 770 contributing to the effect of subsequently externally added substrates and inhibitors. In contrast
 771 to the original protocol, an alternative sequence of titration steps is frequently applied, in which
 772 the alternative ‘State 2’ has an entirely different meaning, when this second state is induced by
 773 addition of fuel substrate without ADP (LEAK-state; in contrast to State 2 defined in **Table 1**
 774 as a ROX state), followed by addition of ADP.

775 **State 3** is the state stimulated by addition of fuel substrates while the ADP concentration
 776 is still high (**Table 3**) and supports coupled energy transformation through oxidative
 777 phosphorylation. ‘High ADP’ is a concentration of ADP specifically selected to allow the
 778 measurement of State 3 to State 4 transitions of isolated mitochondria in a closed respirometric
 779 chamber. Repeated ADP titration re-establishes State 3 at ‘high ADP’. Starting at O_2
 780 concentrations near air-saturation (ca. 200 μM O_2 at sea level and 37 °C), the total ADP
 781 concentration added must be low enough (typically 100 to 300 μM) to allow phosphorylation
 782 to ATP at a coupled O_2 flux that does not lead to O_2 depletion during the transition to State 4.
 783 In contrast, kinetically-saturating ADP concentrations usually are 10-fold higher than ‘high
 784 ADP’, *e.g.*, 2.5 mM in isolated mitochondria. The abbreviation State 3u is occasionally used in
 785 bioenergetics, to indicate the state of respiration after titration of an uncoupler, without
 786 sufficient emphasis on the fundamental difference between OXPHOS-capacity (*well-coupled*
 787 with an *endogenous* uncoupled component) and ET-capacity (*noncoupled*).

788 **State 4** is a LEAK-state that is obtained only if the mitochondrial preparation is intact
 789 and well-coupled. Depletion of ADP by phosphorylation to ATP leads to a decline of O_2 flux
 790 in the transition from State 3 to State 4. Under these conditions of State 4, a maximum
 791 protonmotive force and high ATP/ADP ratio are maintained. For calculation of P_{\gg}/O_2 ratios the
 792 gradual decline of Y_{P_{\gg}/O_2} towards diminishing $[\text{ADP}]$ at State 4 must be taken into account
 793 (Gnaiger 2001). State 4 respiration, L_T (**Table 1**), reflects intrinsic proton leak and intrinsic
 794 ATP hydrolysis activity. O_2 flux in State 4 is an overestimation of LEAK-respiration if the
 795 contaminating ATP hydrolysis activity recycles some ATP to ADP, $J_{P_{\ll}}$, which stimulates
 796 respiration coupled to phosphorylation, $J_{P_{\gg}} > 0$. This can be tested by inhibition of the
 797 phosphorylation-pathway using oligomycin, ensuring that $J_{P_{\gg}} = 0$ (State 4o). Alternatively,
 798 sequential ADP titrations re-establish State 3, followed by State 3 to State 4 transitions while
 799 sufficient O_2 is available. Anoxia may be reached, however, before exhaustion of ADP (State
 800 5).

801 **State 5** is the state after exhaustion of O_2 in a closed respirometric chamber. Diffusion of
 802 O_2 from the surroundings into the aqueous solution may be a confounding factor preventing
 803 complete anoxia (Gnaiger 2001). Chance and Williams (1955) provide an alternative definition
 804 of State 5, which gives it the different meaning of ROX versus anoxia: ‘State 5 may be obtained
 805 by antimycin A treatment or by anaerobiosis’.

806 In **Table 3**, only States 3 and 4 (and ‘State 2’ in the alternative protocol: addition of fuel
 807 substrates without ADP; not included in the table) are coupling control states, with the
 808 restriction that O_2 flux in State 3 may be limited kinetically by non-saturating ADP
 809 concentrations (**Table 1**).

810

811 3. Normalization: fluxes and flows

812

813 3.1. Normalization: system or sample

814

815 The term *rate* is not sufficiently defined to be useful for reporting data (Fig. 6). The
 816 inconsistency of the meanings of rate becomes fully apparent when considering Galileo
 817 Galilei's famous principle, that 'bodies of different weight all fall at the same rate (have a
 818 constant acceleration)' (Coopersmith 2010).

819

820 **Fig. 6. Different meanings of rate may lead to confusion, if the normalization is not**
 821 **sufficiently specified.** Results are frequently expressed as mass-
 822 specific flux, J_{mX} , per mg protein, dry or wet weight (mass). Cell
 823 volume, V_{cell} , may be used for normalization (volume-specific
 824 flux, $J_{V\text{cell}}$), which must be clearly distinguished from flow per cell,
 825 $I_{N\text{cell}}$, or flux, J_V , expressed for methodological reasons per
 826 volume of the measurement system. For details see Table 4.

827

828 **Flow per system, I :** In a generalization of electrical terms, flow as an extensive quantity
 829 (I ; per system) is distinguished from flux as a size-specific quantity (J ; per system size) (Fig.
 830 6). Electric current is flow, I_{el} [$\text{A} \equiv \text{C} \cdot \text{s}^{-1}$] per system (extensive quantity). When dividing this
 831 extensive quantity by system size (cross-sectional area of a 'wire'), a size-specific quantity is
 832 obtained, which is flux (current density), J_{el} [$\text{A} \cdot \text{m}^{-2} = \text{C} \cdot \text{s}^{-1} \cdot \text{m}^{-2}$].

833 **Extensive quantities:** An extensive quantity increases proportionally with system size.
 834 The magnitude of an extensive quantity is completely additive for non-interacting
 835 subsystems—such as mass or flow expressed per defined system. The magnitude of these
 836 quantities depends on the extent or size of the system (Cohen *et al.* 2008).

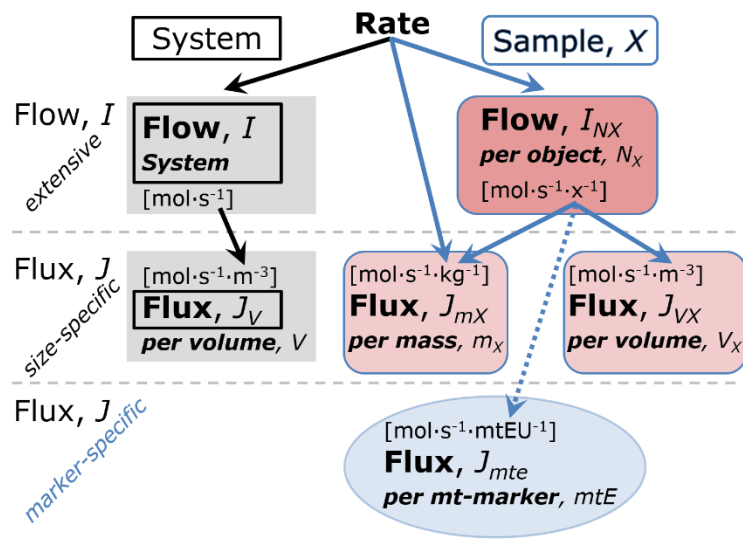
837 **Size-specific quantities:** 'The adjective *specific* before the name of an extensive quantity
 838 is often used to mean *divided by mass*' (Cohen *et al.* 2008). In this system-paradigm, mass-
 839 specific flux is flow divided by mass of the *system* (the total mass of everything within the
 840 measuring chamber or reactor). A mass-specific quantity is independent of the extent of non-
 841 interacting homogenous subsystems. Tissue-specific quantities (related to the *sample* in
 842 contrast to the *system*) are of fundamental interest in comparative mitochondrial physiology,
 843 where *specific* refers to the *type of the sample* rather than *mass of the system*. The term *specific*,
 844 therefore, must be clarified; *sample-specific*, e.g., muscle mass-specific normalization, is
 845 distinguished from *system-specific* quantities (mass or volume; Fig. 6).

846

855 **Box 2: Metabolic fluxes and flows: vectorial and scalar**

856

857 Fluxes are *vectors*, if they have *spatial* geometric direction in addition to magnitude.
 858 Electric charge per unit time is electric flow or current, $I_{\text{el}} = dQ_{\text{el}} \cdot dt^{-1}$ [A]. When expressed per
 859 unit cross-sectional area, A [m^2], a vector flux is obtained, which is current density or surface-
 860 density of flow) perpendicular to the direction of flux, $J_{\text{el}} = I_{\text{el}} \cdot A^{-1}$ [$\text{A} \cdot \text{m}^{-2}$] (Cohen *et al.* 2008).
 861 For all transformations *flows*, I_{tr} , are defined as extensive quantities. Vector and scalar *fluxes*



862 are obtained as $J_{tr} = I_{tr} \cdot A^{-1}$ [$\text{mol} \cdot \text{s}^{-1} \cdot \text{m}^{-2}$] and $J_{tr} = I_{tr} \cdot V^{-1}$ [$\text{mol} \cdot \text{s}^{-1} \cdot \text{m}^{-3}$], expressing flux as an area-
 863 specific vector or volume-specific vectorial or scalar quantity, respectively (Gnaiger 1993b).

864 We suggest to define: (1) *vectorial* fluxes, which are translocations as functions of
 865 *gradients* with direction in geometric space in continuous systems; (2) *vectorial* fluxes, which
 866 describe translocations in discontinuous systems and are restricted to information on
 867 *compartmental differences* (**Fig. 2**, transmembrane proton flux); and (3) *scalar* fluxes, which
 868 are transformations in a *homogenous* system (**Fig. 2**, catabolic O₂ flux, J_{KO_2}).

869 Vectorial transmembrane proton fluxes, $J_{\text{mH}^+\text{pos}}$ and $J_{\text{mH}^+\text{neg}}$, are analyzed in a
 870 heterogenous compartmental system as a quantity with *directional* but not *spatial* information.
 871 Translocation of protons across the mtIM has a defined direction, either from the negative
 872 compartment (matrix space; negative, neg–compartment) to the positive compartment (inter-
 873 membrane space; positive, pos–compartment) or *vice versa* (**Fig. 2**). The arrows defining the
 874 direction of the translocation between the two compartments may point upwards or downwards,
 875 right or left, without any implication that these are actual directions in space. The pos–
 876 compartment is neither above nor below the neg–compartment in a spatial sense, but can be
 877 visualized arbitrarily in a figure in the upper position (**Fig. 2**). In general, the *compartmental*
 878 *direction* of vectorial translocation from the neg–compartment to the pos–compartment is
 879 defined by assigning the initial and final state as *ergodynamic compartments*, $\text{H}^+_{\text{neg}} \rightarrow \text{H}^+_{\text{pos}}$ or
 880 $0 = -1 \text{H}^+_{\text{neg}} + 1 \text{H}^+_{\text{pos}}$, related to work (erg = work) that must be performed to lift the proton from
 881 a lower to a higher electrochemical potential or from the lower to the higher ergodynamic
 882 compartment (Gnaiger 1993b).

883 In analogy to *vectorial* translocation, the direction of a *scalar* chemical reaction, $\text{A} \rightarrow \text{B}$
 884 or $0 = -1 \text{A} + 1 \text{B}$, is defined by assigning substrates and products, A and B, as ergodynamic
 885 compartments. O₂ is defined as a substrate in respiratory O₂ consumption, which together with
 886 the fuel substrates comprises the substrate compartment of the catabolic reaction (**Fig. 2**).
 887 Volume-specific scalar O₂ flux is coupled to vectorial translocation, yielding the $\text{H}^+_{\text{pos}}/\text{O}_2$ ratio
 888 (**Fig. 1**).

889

890

891 3.2. Normalization for system-size: flux per chamber volume

892

893 **System-specific flux, J_{V,O_2} :** The experimental system (experimental chamber) is part of
 894 the measurement apparatus, separated from the environment as an isolated, closed, open,
 895 isothermal or non-isothermal system (**Table 4**). On another level, we distinguish between (1)
 896 the *system* with volume V and mass m defined by the system boundaries, and (2) the *sample* or
 897 *objects* with volume V_X and mass m_X which are enclosed in the experimental chamber (**Fig. 6**).
 898 Metabolic O₂ flow per object, $I_{\text{O}_2/X}$, increases as the mass of the object is increased. Sample
 899 mass-specific O₂ flux, $J_{\text{O}_2/mX}$ should be independent of the mass of the sample studied in the
 900 instrument chamber, but system volume-specific O₂ flux, J_{V,O_2} (per volume of the instrument
 901 chamber), should increase in direct proportion to the mass of the sample in the chamber.
 902 Whereas J_{V,O_2} depends on mass-concentration of the sample in the chamber, it should be
 903 independent of the chamber (system) volume at constant sample mass. There are practical
 904 limitations to increase the mass-concentration of the sample in the chamber, when one is
 905 concerned about crowding effects and instrumental time resolution.

906 When the reactor volume does not change during the reaction, which is typical for liquid
 907 phase reactions, the volume-specific *flux of a chemical reaction* r is the time derivative of the
 908 advancement of the reaction per unit volume, $J_{V,rB} = d_r \zeta_B / dt \cdot V^{-1}$ [$(\text{mol} \cdot \text{s}^{-1}) \cdot \text{L}^{-1}$]. The *rate of*
 909 *concentration change* is dc_B / dt [$(\text{mol} \cdot \text{L}^{-1}) \cdot \text{s}^{-1}$], where concentration is $c_B = n_B / V$. There is a
 910 difference between (1) $J_{V,r\text{O}_2}$ [$\text{mol} \cdot \text{s}^{-1} \cdot \text{L}^{-1}$] and (2) rate of concentration change [$\text{mol} \cdot \text{L}^{-1} \cdot \text{s}^{-1}$].
 911 These merge to a single expression only in closed systems. In open systems, external fluxes
 912 (such as O₂ supply) are distinguished from internal transformations (catabolic flux, O₂

913 consumption). In a closed system, external flows of all substances are zero and O₂ consumption
 914 (internal flow of catabolic reactions k), I_{kO_2} [pmol·s⁻¹], causes a decline of the amount of O₂ in
 915 the system, n_{O_2} [nmol]. Normalization of these quantities for the volume of the system, V [L ≡
 916 dm³], yields volume-specific O₂ flux, $J_{V,kO_2} = I_{kO_2}/V$ [nmol·s⁻¹·L⁻¹], and O₂ concentration, [O₂]
 917 or $c_{O_2} = n_{O_2}/V$ [μmol·L⁻¹ = μM = nmol·mL⁻¹]. Instrumental background O₂ flux is due to external
 918 flux into a non-ideal closed respirometer; then total volume-specific flux has to be corrected for
 919 instrumental background O₂ flux—O₂ diffusion into or out of the instrumental chamber. J_{V,kO_2}
 920 is relevant mainly for methodological reasons and should be compared with the accuracy of
 921 instrumental resolution of background-corrected flux, e.g., ±1 nmol·s⁻¹·L⁻¹ (Gnaiger 2001).
 922 ‘Metabolic’ or catabolic indicates O₂ flux, J_{kO_2} , corrected for: (1) instrumental background O₂
 923 flux; (2) chemical background O₂ flux due to autoxidation of chemical components added to
 924 the incubation medium; and (3) R_{ox} for O₂-consuming side reactions unrelated to the catabolic
 925 pathway k .

926

927 3.3. Normalization: per sample

928

929 The challenges of measuring mitochondrial respiratory flux are matched by those of
 930 normalization. Application of common and defined units is required for direct transfer of
 931 reported results into a database. The second [s] is the *SI* unit for the base quantity *time*. It is also
 932 the standard time-unit used in solution chemical kinetics. A rate may be considered as the
 933 numerator and normalization as the complementary denominator, which are tightly linked in
 934 reporting the measurements in a format commensurate with the requirements of a database.
 935 Normalization (Table 4) is guided by physicochemical principles, methodological
 936 considerations, and conceptual strategies (Fig. 7).

937 **Sample concentration, C_{mX} :** Normalization for sample concentration is required to
 938 report respiratory data. Considering a tissue or cells as the sample, X , the sample mass is m_X
 939 [mg], which is frequently measured as wet or dry weight, W_w or W_d [mg], or as amount of tissue
 940 or cell protein, m_{Protein} . In the case of permeabilized tissues, cells, and homogenates, the sample
 941 concentration, $C_{mX} = m_X/V$ [g·L⁻¹ = mg·mL⁻¹], is the mass of the subsample of tissue that is
 942 transferred into the instrument chamber.

943 **Mass-specific flux, $J_{O_2/mX}$:** Mass-specific flux is obtained by expressing respiration per
 944 mass of sample, m_X [mg]. X is the type of sample—isolated mitochondria, tissue homogenate,
 945 permeabilized fibres or cells. Volume-specific flux is divided by mass concentration of X , $J_{O_2/mX}$
 946 = $J_{V,O_2}/C_{mX}$; or flow per cell is divided by mass per cell, $J_{O_2/mcell} = I_{O_2/cell}/M_{cell}$. If mass-specific
 947 O₂ flux is constant and independent of sample size (expressed as mass), then there is no
 948 interaction between the subsystems. A 1.5 mg and a 3.0 mg muscle sample respire at identical
 949 mass-specific flux. Mass-specific O₂ flux, however, may change with the mass of a tissue
 950 sample, cells or isolated mitochondria in the measuring chamber, in which the nature of the
 951 interaction becomes an issue. Therefore, cell density must be optimized, particularly in
 952 experiments carried out in wells, considering the confluency of the cell monolayer or clumps
 953 of cells (Salabei *et al.* 2014).

954 **Number concentration, C_{NX} :** C_{NX} is the experimental *number concentration* of sample
 955 X . In the case of cells or animals, e.g., nematodes, $C_{NX} = N_X/V$ [X·L⁻¹], where N_X is the number
 956 of cells or organisms in the chamber (Table 4).

957 **Flow per object, $I_{O_2/X}$:** A special case of normalization is encountered in respiratory
 958 studies with permeabilized (or intact) cells. If respiration is expressed per cell, the O₂ flow per
 959 measurement system is replaced by the O₂ flow per cell, $I_{O_2/cell}$ (Table 4). O₂ flow can be
 960 calculated from volume-specific O₂ flux, J_{V,O_2} [nmol·s⁻¹·L⁻¹] (per V of the measurement chamber
 961 [L]), divided by the number concentration of cells, $C_{Ncell} = N_{cell}/V$ [cell·L⁻¹], where N_{cell} is the
 962 number of cells in the chamber. The total cell count is the sum of viable and dead cells, $N_{cell} =$
 963 $N_{vce} + N_{dce}$ (Table 5). The cell viability index, $CVI = N_{vce}/N_{cell}$, is the ratio of viable cells (N_{vce} ;

964 before experimental permeabilization) per total cell count. After experimental permeabilization,
 965 all cells are permeabilized, $N_{pce} = N_{cell}$. The cell viability index can be used to normalize
 966 respiration for the number of cells that have been viable before experimental permeabilization,
 967 $I_{O_2/vce} = I_{O_2/cell}/CVI$, considering that mitochondrial respiratory dysfunction in dead cells should
 968 be eliminated as a confounding factor.

969 Cellular O_2 flow can be compared between cells of identical size. To take into account
 970 changes and differences in cell size, normalization is required to obtain cell size-specific or
 971 mitochondrial marker-specific O_2 flux (Renner *et al.* 2003).

972 The complexity changes when the sample is a whole organism studied as an experimental
 973 model. The scaling law in respiratory physiology reveals a strong interaction of O_2 flow and
 974 individual body mass of an organism, since *basal* metabolic rate (flow) does not increase
 975 linearly with body mass, whereas *maximum* mass-specific O_2 flux, \dot{V}_{O_2max} or \dot{V}_{O_2peak} , is
 976 approximately constant across a large range of individual body mass (Weibel and Hoppeler
 977 2005), with individuals, breeds, and species deviating substantially from this relationship.
 978 \dot{V}_{O_2peak} of human endurance athletes is 60 to 80 mL $O_2 \cdot \text{min}^{-1} \cdot \text{kg}^{-1}$ body mass, converted to
 979 $J_{O_2peak/M}$ of 45 to 60 $\text{nmol} \cdot \text{s}^{-1} \cdot \text{g}^{-1}$ (Gnaiger 2014; **Table 6**).

980
 981
 982

Table 4. Sample concentrations and normalization of flux.

Expression	Symbol	Definition	Unit	Notes
Sample				
identity of sample	X	object: cell, tissue, animal, patient		
number of sample entities X	N_X	number of objects	x	
mass of sample X	m_X		kg	1
mass of object X	M_X	$M_X = m_X \cdot N_X^{-1}$	$\text{kg} \cdot \text{x}^{-1}$	1
Mitochondria				
Mitochondria	mt	$X = \text{mt}$		
amount of mt-elements	mtE	quantity of mt-marker	mtEU	
Concentrations				
object number concentration	C_{NX}	$C_{NX} = N_X \cdot V^{-1}$	$\text{x} \cdot \text{m}^{-3}$	2
sample mass concentration	C_{mX}	$C_{mX} = m_X \cdot V^{-1}$	$\text{kg} \cdot \text{m}^{-3}$	
mitochondrial concentration	C_{mtE}	$C_{mtE} = mtE \cdot V^{-1}$	$\text{mtEU} \cdot \text{m}^{-3}$	3
specific mitochondrial density	D_{mtE}	$D_{mtE} = mtE \cdot m_X^{-1}$	$\text{mtEU} \cdot \text{kg}^{-1}$	4
mitochondrial content, mtE per object X	mtE_X	$mtE_X = mtE \cdot N_X^{-1}$	$\text{mtEU} \cdot \text{x}^{-1}$	5
O_2 flow and flux				
flow, system	I_{O_2}	internal flow	$\text{mol} \cdot \text{s}^{-1}$	6
volume-specific flux	J_{V,O_2}	$J_{V,O_2} = I_{O_2} \cdot V^{-1}$	$\text{mol} \cdot \text{s}^{-1} \cdot \text{m}^{-3}$	7
flow per object X	$I_{O_2/X}$	$I_{O_2/X} = J_{V,O_2} \cdot C_{NX}^{-1}$	$\text{mol} \cdot \text{s}^{-1} \cdot \text{x}^{-1}$	8
mass-specific flux	$J_{O_2/mX}$	$J_{O_2/mX} = J_{V,O_2} \cdot C_{mX}^{-1}$	$\text{mol} \cdot \text{s}^{-1} \cdot \text{kg}^{-1}$	9
mitochondria-specific flux	$J_{O_2/mtE}$	$J_{O_2/mtE} = J_{V,O_2} \cdot C_{mtE}^{-1}$	$\text{mol} \cdot \text{s}^{-1} \cdot \text{mtEU}^{-1}$	10

983 1 The *S/* prefix k is used for the SI base unit of mass ($\text{kg} = 1,000 \text{ g}$). In praxis, various *S/* prefixes are
 984 used for convenience, to make numbers easily readable, e.g., 1 mg tissue, cell or mitochondrial mass
 985 instead of 0.000001 kg.

986 2 In case sample $X = \text{cells}$, the object number concentration is $C_{Ncell} = N_{cell} \cdot V^{-1}$, and volume may be
 987 expressed in [$\text{dm}^3 \equiv \text{L}$] or [$\text{cm}^3 = \text{mL}$]. See **Table 5** for different object types.

- 988 3 mt-concentration is an experimental variable, dependent on sample concentration: (1) $C_{mtE} = mtE \cdot V^{-1}$;
989 (2) $C_{mtE} = mtE_X \cdot C_{NX}$; (3) $C_{mtE} = C_{mX} \cdot D_{mtE}$.
990 4 If the amount of mitochondria, mtE , is expressed as mitochondrial mass, then D_{mtE} is the mass
991 fraction of mitochondria in the sample. If mtE is expressed as mitochondrial volume, V_{mt} , and the
992 mass of sample, m_X , is replaced by volume of sample, V_X , then D_{mtE} is the volume fraction of
993 mitochondria in the sample.
994 5 $mtE_X = mtE \cdot N_X^{-1} = C_{mtE} \cdot C_{NX}^{-1}$.
995 6 O_2 can be replaced by other chemicals B to study different reactions, e.g., ATP, H_2O_2 , or
996 compartmental translocations, e.g., Ca^{2+} .
997 7 I_{O_2} and V are defined per instrument chamber as a system of constant volume (and constant
998 temperature), which may be closed or open. I_{O_2} is abbreviated for I_{rO_2} , i.e., the metabolic or internal
999 O_2 flow of the chemical reaction r in which O_2 is consumed, hence the negative stoichiometric
1000 number, $\nu_{O_2} = -1$. $I_{rO_2} = d_r n_{O_2} / dt \cdot \nu_{O_2}^{-1}$. If r includes all chemical reactions in which O_2 participates, then
1001 $d_r n_{O_2} = dn_{O_2} - d_e n_{O_2}$, where dn_{O_2} is the change in the amount of O_2 in the instrument chamber and $d_e n_{O_2}$
1002 is the amount of O_2 added externally to the system. At steady state, by definition $dn_{O_2} = 0$, hence $d_r n_{O_2}$
1003 $= -d_e n_{O_2}$.
1004 8 J_{V,O_2} is an experimental variable, expressed per volume of the instrument chamber.
1005 9 I_{O_2X} is a physiological variable, depending on the size of entity X .
1006 10 There are many ways to normalize for a mitochondrial marker, that are used in different experimental
1007 approaches: (1) $J_{O_2/mtE} = J_{V,O_2} \cdot C_{mtE}^{-1}$; (2) $J_{O_2/mtE} = J_{V,O_2} \cdot C_{mX}^{-1} \cdot D_{mtE}^{-1} = J_{O_2/mX} \cdot D_{mtE}^{-1}$; (3) $J_{O_2/mtE} =$
1008 $J_{V,O_2} \cdot C_{NX}^{-1} \cdot mtE_X^{-1} = I_{O_2X} \cdot mtE_X^{-1}$; (4) $J_{O_2/mtE} = I_{O_2} \cdot mtE^{-1}$. The mt-elemental unit [mtEU] varies between
1009 different mt-markers.
1010
1011

Table 5. Sample types, X, abbreviations, and quantification.

Identity of sample	X	N_X	Mass ^a	Volume	mt-Marker
mitochondrial preparation	mt-prep	[x]	[kg]	[m ³]	[mtEU]
isolated mitochondria	imt		m_{mt}	V_{mt}	mtE
tissue homogenate	thom		m_{thom}		mtE_{thom}
permeabilized tissue	pti		m_{pti}		mtE_{pti}
permeabilized fibre	pfi		m_{pfi}		mtE_{pfi}
permeabilized cell	pce	N_{pce}	M_{pce}	V_{pce}	mtE_{pce}
cells ^b	cell	N_{cell}	M_{cell}	V_{cell}	mtE_{cell}
intact cell, viable cell	vce	N_{vce}	M_{vce}	V_{vce}	
dead cell	dce	N_{dce}	M_{dce}	V_{dce}	
Organism	org	N_{org}	M_{org}	V_{org}	

^a Instead of mass, frequently the wet weight or dry weight is stated, W_w or W_d .
 m_X is mass of the sample [kg], M_X is mass of the object [kg·x⁻¹].

^b Total cell count, $N_{cell} = N_{vce} + N_{dce}$

3.4. Normalization for mitochondrial content

Tissues can contain multiple cell populations that may have distinct mitochondrial subtypes. Mitochondria undergo dynamic fission and fusion cycles, and can exist in multiple stages and sizes which may be altered by a range of factors. The isolation of mitochondria (often achieved through differential centrifugation) can therefore yield a subsample of the mitochondrial types present in a tissue, depending on isolation protocols utilized (e.g., centrifugation speed). This possible bias should be taken into account when planning experiments using isolated mitochondria. Different sizes of mitochondria are enriched at specific centrifugation speeds, which can be used strategically for isolation of mitochondrial subpopulations.

Part of the mitochondrial content of a tissue is lost during preparation of isolated mitochondria. The fraction of mitochondria in the isolate is expressed as mitochondrial recovery. At a high mitochondrial recovery the sample of isolated mitochondria is more representative of the total mitochondrial population than in preparations characterized by low recovery. Determination of the mitochondrial recovery and yield is based on measurement of

1032 the concentration of a mitochondrial marker in the tissue homogenate, $C_{mtE,thom}$, which
 1033 simultaneously provides information on the specific mitochondrial density in the sample.
 1034

Flow, Performance	=	Element function	x	Element density	x	Size of object
$\frac{\text{mol}\cdot\text{s}^{-1}}{x}$	=	$\frac{\text{mol}\cdot\text{s}^{-1}}{x_{mtE}}$	·	$\frac{x_{mtE}}{\text{kg}}$	·	$\frac{\text{kg}}{x}$

A	Flow	=	mt-specific flux	x	mt-structure, functional elements
	$I_{O_2/X}$	=	$J_{O_2/mtE}$	·	mtE_X
					$\frac{mtE_X}{M_X} \cdot M_X$

$I_{O_2/X}$	=	$J_{O_2/mtE}$	·	D_{mtE}	·	M_X
$\frac{I_{O_2/X}}{M_X}$	=	$\frac{I_{O_2/X}}{mtE_X}$	·	$\frac{mtE_X}{M_X}$		

B	Flow	=	Object mass- specific flux	x	Mass of object
	$I_{O_2/X}$	=	$J_{O_2/MX}$	·	M_X

1035 **Fig. 7. Structure-function analysis of performance of an organism, organ or tissue, or a**
 1036 **cell (sample entity, X). O₂ flow, $I_{O_2/X}$, is the product of performance per functional element**
 1037 **(element function, mitochondria-specific flux), element density (mitochondrial density,**
 1038 **D_{mtE}), and size of entity X (mass, M_X). (A) Structured analysis: performance is the product of**
 1039 **mitochondrial function (mt-specific flux) and structure (functional elements; D_{mtE} times mass**
 1040 **of X). (B) Unstructured analysis: performance is the product of entity mass-specific flux, $J_{O_2/MX}$**
 1041 **$= I_{O_2/X}/M_X = I_{O_2/mx}$ [mol·s⁻¹·kg⁻¹] and size of entity, expressed as mass of X; $M_X = m_X \cdot N_X^{-1}$**
 1042 **[kg·x⁻¹]. See Table 4 for further explanation of quantities and units. Modified from Gnaiger**
 1043 **(2014).**
 1044
 1045

1046 Normalization is a problematic subject; it is essential to consider the question of the study.
 1047 If the study aims at comparing tissue performance—such as the effects of a treatment on a
 1048 specific tissue, then normalization can be successful, using tissue mass or protein content, for
 1049 example. However, if the aim is to find differences on mitochondrial function independent of
 1050 mitochondrial density (Table 4), then normalization to a mitochondrial marker is imperative
 1051 (Fig. 7). One cannot assume that quantitative changes in various markers—such as
 1052 mitochondrial proteins—necessarily occur in parallel with one another. It should be established
 1053 that the marker chosen is not selectively altered by the performed treatment. In conclusion, the
 1054 normalization must reflect the question under investigation to reach a satisfying answer. On the
 1055 other hand, the goal of comparing results across projects and institutions requires
 1056 standardization on normalization for entry into a databank.

1057 **Mitochondrial concentration, C_{mtE} , and mitochondrial markers:** Mitochondrial
 1058 organelles comprise a dynamic cellular reticulum in various states of fusion and fission. Hence,
 1059 the definition of an "amount" of mitochondria is often misconceived: mitochondria cannot be
 1060 counted reliably as a number of occurring elements. Therefore, quantification of the "amount"
 1061 of mitochondria depends on the measurement of chosen mitochondrial markers. 'Mitochondria
 1062 are the structural and functional elemental units of cell respiration' (Gnaiger 2014). The
 1063 quantity of a mitochondrial marker can reflect the amount of *mitochondrial elements*, *mtE*,
 1064 expressed in various mitochondrial elemental units [mtEU] specific for each measured mt-

1065 marker (**Table 4**). However, since mitochondrial quality may change in response to stimuli—
 1066 particularly in mitochondrial dysfunction and after exercise training (Pesta *et al.* 2011; Campos
 1067 *et al.* 2017)—some markers can vary while others are unchanged: (1) Mitochondrial volume
 1068 and membrane area are structural markers, whereas mitochondrial protein mass is frequently
 1069 used as a marker for isolated mitochondria. (2) Molecular and enzymatic mitochondrial markers
 1070 (amounts or activities) can be selected as matrix markers, *e.g.*, citrate synthase activity, mtDNA;
 1071 mtIM-markers, *e.g.*, cytochrome *c* oxidase activity, *aa3* content, cardiolipin, or mtOM-markers,
 1072 *e.g.*, TOM20. (3) Extending the measurement of mitochondrial marker enzyme activity to
 1073 mitochondrial pathway capacity, ET- or OXPHOS-capacity can be considered as an integrative
 1074 functional mitochondrial marker.

1075 Depending on the type of mitochondrial marker, the mitochondrial elements, *mtE*, are
 1076 expressed in marker-specific units. Mitochondrial concentration in the measurement chamber
 1077 and the tissue of origin are quantified as (1) a quantity for normalization in functional analyses,
 1078 C_{mtE} , and (2) a physiological output that is the result of mitochondrial biogenesis and
 1079 degradation, D_{mtE} , respectively (**Table 4**). It is recommended, therefore, to distinguish
 1080 *experimental mitochondrial concentration*, $C_{mtE} = mtE/V$ and *physiological mitochondrial*
 1081 *density*, $D_{mtE} = mtE/m_X$. Then mitochondrial density is the amount of mitochondrial elements
 1082 per mass of tissue, which is a biological variable (**Fig. 7**). The experimental variable is
 1083 mitochondrial density multiplied by sample mass concentration in the measuring chamber, C_{mtE}
 1084 $= D_{mtE} \cdot C_{mX}$, or mitochondrial content multiplied by sample number concentration, $C_{mtE} =$
 1085 $mtE_X \cdot C_{NX}$ (**Table 4**).

1086 **Mitochondria-specific flux, $J_{O_2/mtE}$** : Volume-specific metabolic O_2 flux depends on: (1)
 1087 the sample concentration in the volume of the instrument chamber, C_{mX} , or C_{NX} ; (2) the
 1088 mitochondrial density in the sample, $D_{mtE} = mtE/m_X$ or $mtE_X = mtE/N_X$; and (3) the specific
 1089 mitochondrial activity or performance per elemental mitochondrial unit, $J_{O_2/mtE} = J_{V,O_2}/C_{mtE}$
 1090 [$\text{mol} \cdot \text{s}^{-1} \cdot \text{mtEU}^{-1}$] (**Table 4**). Obviously, the numerical results for $J_{O_2/mtE}$ vary with the type of
 1091 mitochondrial marker chosen for measurement of *mtE* and $C_{mtE} = mtE/V$ [$\text{mtEU} \cdot \text{m}^{-3}$].

1092

1093 3.5. Evaluation of mitochondrial markers

1094

1095 Different methods are implicated in the quantification of mitochondrial markers and have
 1096 different strengths. Some problems are common for all mitochondrial markers, *mtE*: (1)
 1097 Accuracy of measurement is crucial, since even a highly accurate and reproducible
 1098 measurement of O_2 flux results in an inaccurate and noisy expression normalized for a biased
 1099 and noisy measurement of a mitochondrial marker. This problem is acute in mitochondrial
 1100 respiration because the denominators used (the mitochondrial markers) are often small moieties
 1101 of which accurate and precise determination is difficult. This problem can be avoided when O_2
 1102 fluxes measured in substrate-uncoupler-inhibitor titration protocols are normalized for flux in
 1103 a defined respiratory reference state, which is used as an *internal* marker and yields flux control
 1104 ratios, *FCRs*. *FCRs* are independent of *externally* measured markers and, therefore, are
 1105 statistically robust, considering the limitations of ratios in general (Jasienski and Bazzaz 1999).
 1106 *FCRs* indicate qualitative changes of mitochondrial respiratory control, with highest
 1107 quantitative resolution, separating the effect of mitochondrial density or concentration on $J_{O_2/mX}$
 1108 and $I_{O_2/X}$ from that of function per elemental mitochondrial marker, $J_{O_2/mtE}$ (Pesta *et al.* 2011;
 1109 Gnaiger 2014). (2) If mitochondrial quality does not change and only the amount of
 1110 mitochondria varies as a determinant of mass-specific flux, any marker is equally qualified in
 1111 principle; then in practice selection of the optimum marker depends only on the accuracy and
 1112 precision of measurement of the mitochondrial marker. (3) If mitochondrial flux control ratios
 1113 change, then there may not be any best mitochondrial marker. In general, measurement of
 1114 multiple mitochondrial markers enables a comparison and evaluation of normalization for a
 1115 variety of mitochondrial markers. Particularly during postnatal development, the activity of

1116 marker enzymes—such as cytochrome *c* oxidase and citrate synthase—follows different time
 1117 courses (Drahota *et al.* 2004). Evaluation of mitochondrial markers in healthy controls is
 1118 insufficient for providing guidelines for application in the diagnosis of pathological states and
 1119 specific treatments.

1120 In line with the concept of the respiratory control ratio (Chance and Williams 1955a), the
 1121 most readily used normalization is that of flux control ratios and flux control factors (Gnaiger
 1122 2014). Selection of the state of maximum flux in a protocol as the reference state has the
 1123 advantages of: (1) internal normalization; (2) statistical linearization of the response in the range
 1124 of 0 to 1; and (3) consideration of maximum flux for integrating a large number of elemental
 1125 steps in the OXPHOS- or ET-pathways. This reduces the risk of selecting a functional marker
 1126 that is specifically altered by the treatment or pathology, yet increases the chance that the highly
 1127 integrative pathway is disproportionately affected, *e.g.*, the OXPHOS- rather than ET-pathway
 1128 in case of an enzymatic defect in the phosphorylation-pathway. In this case, additional
 1129 information can be obtained by reporting flux control ratios based on a reference state which
 1130 indicates stable tissue-mass specific flux. Stereological determination of mitochondrial content
 1131 via two-dimensional transmission electron microscopy can have limitations due to the dynamics
 1132 of mitochondrial size (Meinild Lundby *et al.* 2017). Accurate determination of three-
 1133 dimensional volume by two-dimensional microscopy can be both time consuming and
 1134 statistically challenging (Larsen *et al.* 2012).

1135 The validity of using mitochondrial marker enzymes (citrate synthase activity, Complex
 1136 I–IV amount or activity) for normalization of flux is limited in part by the same factors that
 1137 apply to flux control ratios. Strong correlations between various mitochondrial markers and
 1138 citrate synthase activity (Reichmann *et al.* 1985; Boushel *et al.* 2007; Mogensen *et al.* 2007)
 1139 are expected in a specific tissue of healthy subjects and in disease states not specifically
 1140 targeting citrate synthase. Citrate synthase activity is acutely modifiable by exercise
 1141 (Tonkonogi *et al.* 1997; Leek *et al.* 2001). Evaluation of mitochondrial markers related to a
 1142 selected age and sex cohort cannot be extrapolated to provide recommendations for
 1143 normalization in respirometric diagnosis of disease, in different states of development and
 1144 ageing, different cell types, tissues, and species. mtDNA normalized to nDNA via qPCR is
 1145 correlated to functional mitochondrial markers including OXPHOS- and ET-capacity in some
 1146 cases (Puntschart *et al.* 1995; Wang *et al.* 1999; Menshikova *et al.* 2006; Boushel *et al.* 2007),
 1147 but lack of such correlations have been reported (Menshikova *et al.* 2005; Schultz and Wiesner
 1148 2000; Pesta *et al.* 2011). Several studies indicate a strong correlation between cardiolipin
 1149 content and increase in mitochondrial function with exercise (Menshikova *et al.* 2005;
 1150 Menshikova *et al.* 2007; Larsen *et al.* 2012; Faber *et al.* 2014), but its use as a general
 1151 mitochondrial biomarker in disease remains questionable.

1152

1153 3.6. Conversion: units

1154

1155 Many different units have been used to report the O₂ consumption rate, OCR (**Table 6**).
 1156 *SI* base units provide the common reference to introduce the theoretical principles (**Fig. 6**), and
 1157 are used with appropriately chosen *SI* prefixes to express numerical data in the most practical
 1158 format, with an effort towards unification within specific areas of application (**Table 7**).
 1159 Reporting data in *SI* units—including the mole [mol], coulomb [C], joule [J], and second [s]—
 1160 should be encouraged, particularly by journals which propose the use of *SI* units.

1161 Although volume is expressed as m³ using the *SI* base unit, the litre [dm³] is a
 1162 conventional unit of volume for concentration and is used for most solution chemical kinetics.
 1163 If one multiplies $I_{O_2/cell}$ by $C_{N_{cell}}$, then the result will not only be the amount of O₂ [mol]
 1164 consumed per time [s⁻¹] in one litre [L⁻¹], but also the change in O₂ concentration per second
 1165 (for any volume of an ideally closed system). This is ideal for kinetic modeling as it blends with
 1166 chemical rate equations where concentrations are typically expressed in mol·L⁻¹ (Wagner *et al.*

1167 2011). In studies of multinuclear cells—such as differentiated skeletal muscle cells—it is easy
 1168 to determine the number of nuclei but not the total number of cells. A generalized concept,
 1169 therefore, is obtained by substituting cells by nuclei as the sample entity. This does not hold,
 1170 however, for enucleated platelets.

1171
 1172
 1173
 1174
 1175

Table 6. Conversion of various units used in respirometry and ergometry. e^- is the number of electrons or reducing equivalents. z_B is the charge number of entity B.

1 Unit	x	Multiplication factor	SI-unit	Note
ng.atom O·s ⁻¹	(2 e ⁻)	0.5	nmol O ₂ ·s ⁻¹	
ng.atom O·min ⁻¹	(2 e ⁻)	8.33	pmol O ₂ ·s ⁻¹	
natom O·min ⁻¹	(2 e ⁻)	8.33	pmol O ₂ ·s ⁻¹	
nmol O ₂ ·min ⁻¹	(4 e ⁻)	16.67	pmol O ₂ ·s ⁻¹	
nmol O ₂ ·h ⁻¹	(4 e ⁻)	0.2778	pmol O ₂ ·s ⁻¹	
mL O ₂ ·min ⁻¹ at STPD ^a		0.744	μmol O ₂ ·s ⁻¹	1
W = J/s at -470 kJ/mol O ₂		-2.128	μmol O ₂ ·s ⁻¹	
mA = mC·s ⁻¹	(z _{H+} = 1)	10.36	nmol H ⁺ ·s ⁻¹	2
mA = mC·s ⁻¹	(z _{O₂} = 4)	2.59	nmol O ₂ ·s ⁻¹	2
nmol H ⁺ ·s ⁻¹	(z _{H+} = 1)	0.09649	mA	3
nmol O ₂ ·s ⁻¹	(z _{O₂} = 4)	0.38594	mA	3

- 1176 1 At standard temperature and pressure dry (STPD: 0 °C = 273.15 K and 1 atm =
 1177 101.325 kPa = 760 mmHg), the molar volume of an ideal gas, V_m , and V_{m,O_2} is
 1178 22.414 and 22.392 L·mol⁻¹, respectively. Rounded to three decimal places, both
 1179 values yield the conversion factor of 0.744. For comparison at NTPD (20 °C),
 1180 V_{m,O_2} is 24.038 L·mol⁻¹. Note that the SI standard pressure is 100 kPa.
 1181 2 The multiplication factor is $10^6/(z_B \cdot F)$.
 1182 3 The multiplication factor is $z_B \cdot F/10^6$.

1183

1184 For studies of cells, we recommend that respiration be expressed, as far as possible, as:
 1185 (1) O₂ flux normalized for a mitochondrial marker, for separation of the effects of mitochondrial
 1186 quality and content on cell respiration (this includes FCRs as a normalization for a functional
 1187 mitochondrial marker); (2) O₂ flux in units of cell volume or mass, for comparison of respiration
 1188 of cells with different cell size (Renner *et al.* 2003) and with studies on tissue preparations, and
 1189 (3) O₂ flow in units of attomole (10⁻¹⁸ mol) of O₂ consumed in a second by each cell
 1190 [amol·s⁻¹·cell⁻¹], numerically equivalent to [pmol·s⁻¹·10⁻⁶ cells]. This convention allows
 1191 information to be easily used when designing experiments in which O₂ flow must be considered.
 1192 For example, to estimate the volume-specific O₂ flux in an instrument chamber that would be
 1193 expected at a particular cell number concentration, one simply needs to multiply the flow per
 1194 cell by the number of cells per volume of interest. This provides the amount of O₂ [mol]
 1195 consumed per time [s⁻¹] per unit volume [L⁻¹]. At an O₂ flow of 100 amol·s⁻¹·cell⁻¹ and a cell
 1196 density of 10⁹ cells·L⁻¹ (10⁶ cells·mL⁻¹), the volume-specific O₂ flux is 100 nmol·s⁻¹·L⁻¹ (100
 1197 pmol·s⁻¹·mL⁻¹).

1198 ET-capacity in human cell types including HEK 293, primary HUVEC and fibroblasts
 1199 ranges from 50 to 180 amol·s⁻¹·cell⁻¹, measured in intact cells in the noncoupled state (see
 1200 Gnaiger 2014). At 100 amol·s⁻¹·cell⁻¹ corrected for *Rox*, the current across the mt-membranes,
 1201 $I_{H^+e^-}$, approximates 193 pA·cell⁻¹ or 0.2 nA per cell. See Rich (2003) for an extension of
 1202 quantitative bioenergetics from the molecular to the human scale, with a transmembrane proton

1203 flux equivalent to 520 A in an adult at a catabolic power of -110 W. Modelling approaches
 1204 illustrate the link between protonmotive force and currents (Willis *et al.* 2016).

1205

1206

Table 7. Conversion of units with preservation of numerical values.

Name	Frequently used unit	Equivalent unit	Note
volume-specific flux, J_{V,O_2}	$\text{pmol}\cdot\text{s}^{-1}\cdot\text{mL}^{-1}$	$\text{nmol}\cdot\text{s}^{-1}\cdot\text{L}^{-1}$	1
	$\text{mmol}\cdot\text{s}^{-1}\cdot\text{L}^{-1}$	$\text{mol}\cdot\text{s}^{-1}\cdot\text{m}^{-3}$	
cell-specific flow, $I_{O_2/\text{cell}}$	$\text{pmol}\cdot\text{s}^{-1}\cdot 10^{-6}$ cells	$\text{amol}\cdot\text{s}^{-1}\cdot\text{cell}^{-1}$	2
	$\text{pmol}\cdot\text{s}^{-1}\cdot 10^{-9}$ cells	$\text{zmol}\cdot\text{s}^{-1}\cdot\text{cell}^{-1}$	3
cell number concentration, C_{Nce}	10^6 cells $\cdot\text{mL}^{-1}$	10^9 cells $\cdot\text{L}^{-1}$	
mitochondrial protein concentration, C_{mtE}	0.1 mg $\cdot\text{mL}^{-1}$	0.1 g $\cdot\text{L}^{-1}$	
mass-specific flux, $J_{O_2/m}$	$\text{pmol}\cdot\text{s}^{-1}\cdot\text{mg}^{-1}$	$\text{nmol}\cdot\text{s}^{-1}\cdot\text{g}^{-1}$	4
catabolic power, P_k	$\mu\text{W}\cdot 10^{-6}$ cells	$\text{pW}\cdot\text{cell}^{-1}$	1
Volume	1,000 L	m^3 (1,000 kg)	
	L	dm^3 (kg)	
	mL	cm^3 (g)	
	μL	mm^3 (mg)	
	fL	μm^3 (pg)	5
amount of substance concentration	$\text{M} = \text{mol}\cdot\text{L}^{-1}$	$\text{mol}\cdot\text{dm}^{-3}$	

1207

1208 1 pmol: picomole = 10^{-12} mol4 nmol: nanomole = 10^{-9} mol1209 2 amol: attomole = 10^{-18} mol5 fL: femtolitre = 10^{-15} L1210 3 zmol: zeptomole = 10^{-21} mol

1211

1212 We consider isolated mitochondria as powerhouses and proton pumps as molecular
 1213 machines to relate experimental results to energy metabolism of the intact cell. The cellular
 1214 P_{\gg}/O_2 based on oxidation of glycogen is increased by the glycolytic (fermentative) substrate-
 1215 level phosphorylation of 3 P_{\gg}/Glyc or 0.5 mol P_{\gg} for each mol O_2 consumed in the complete
 1216 oxidation of a mol glycosyl unit (Glyc). Adding 0.5 to the mitochondrial P_{\gg}/O_2 ratio of 5.4
 1217 yields a bioenergetic cell physiological P_{\gg}/O_2 ratio close to 6. Two NADH equivalents are
 1218 formed during glycolysis and transported from the cytosol into the mitochondrial matrix, either
 1219 by the malate-aspartate shuttle or by the glycerophosphate shuttle resulting in different
 1220 theoretical yields of ATP generated by mitochondria, the energetic cost of which potentially
 1221 must be taken into account. Considering also substrate-level phosphorylation in the TCA cycle,
 1222 this high P_{\gg}/O_2 ratio not only reflects proton translocation and OXPHOS studied in isolation,
 1223 but integrates mitochondrial physiology with energy transformation in the living cell (Gnaiger
 1224 1993a).

1225

1226

1227 4. Conclusions

1228

1229 MitoEAGLE can serve as a gateway to better diagnose mitochondrial respiratory defects
 1230 linked to genetic variation, age-related health risks, sex-specific mitochondrial performance,
 1231 lifestyle with its effects on degenerative diseases, and thermal and chemical environment. The
 1232 present recommendations on coupling control states and rates, linked to the concept of the
 1233 protonmotive force, are focused on studies with mitochondrial preparations. These will be
 1234 extended in a series of reports on pathway control of mitochondrial respiration, respiratory
 1235 states in intact cells, and harmonization of experimental procedures.

1236

1237
 1238
 1239
 1240
 1241
 1242
 1243
 1244
 1245
 1246
 1247
 1248
 1249
 1250
 1251
 1252
 1253
 1254
 1255
 1256
 1257
 1258
 1259
 1260
 1261
 1262
 1263
 1264
 1265
 1266
 1267
 1268
 1269
 1270
 1271
 1272
 1273
 1274
 1275
 1276
 1277
 1278
 1279
 1280
 1281
 1282
 1283
 1284
 1285
 1286

Box 3: Mitochondrial and cell respiration

Mitochondrial and cell respiration is the process of exergonic and exothermic energy transformation in which scalar redox reactions are coupled to vectorial ion translocation across a semipermeable membrane, which separates the small volume of a bacterial cell or mitochondrion from the larger volume of its surroundings. The electrochemical exergy can be partially conserved in the phosphorylation of ADP to ATP or in ion pumping, or dissipated in an electrochemical short-circuit. Respiration is thus clearly distinguished from fermentation as the counterpart of cellular core energy metabolism. Respiration is separated in mitochondrial preparations from the partial contribution of fermentative pathways of the intact cell. Residual O₂ consumption—as measured after inhibition of mitochondrial electron transfer—does not belong to the class of catabolic reactions and is, therefore, subtracted from total O₂ consumption to obtain baseline-corrected respiration.

Mitochondrial dysfunction is associated with a wide variety of genetic and degenerative diseases. Robust mitochondrial function is supported by physical exercise and caloric balance, and is central for sustained metabolic health throughout life. Therefore, a more consistent presentation of mitochondrial physiology will improve our understanding of the etiology of disease, the diagnostic repertoire of mitochondrial medicine, with a focus on protective medicine, lifestyle and healthy aging.

The optimal choice for expressing mitochondrial and cell respiration (**Box 3**) as O₂ flow per biological sample, and normalization for specific tissue-markers (volume, mass, protein) and mitochondrial markers (volume, protein, content, mtDNA, activity of marker enzymes, respiratory reference state) is guided by the scientific question under study. Interpretation of the data depends critically on appropriate normalization.

We recommend for studies with mitochondrial preparations:

1. Normalization of respiratory rates should be provided as far as possible: (1) biophysical normalization: on a per cell basis as O₂ flow (may not be possible when dealing with tissues); (2) cellular normalization: per g cell or tissue protein, or per cell or tissue mass as mass-specific O₂ flux; and (3) mitochondrial normalization: per mitochondrial marker as mt-specific flux. With information on cell size and the use of multiple normalizations, maximum potential information is available (Renner *et al.* 2003; Wagner *et al.* 2011; Gnaiger 2014). Reporting flow in a respiratory chamber [nmol·s⁻¹] is discouraged, since it restricts the analysis to intra-experimental comparison of relative (qualitative) differences.
2. Catabolic mitochondrial respiration is distinguished from residual oxygen consumption. Fluxes in mitochondrial coupling states should be, as far as possible, corrected for residual oxygen consumption.
3. In studies of isolated mitochondria, the mitochondrial recovery and yield should be reported. Experimental criteria for evaluation of purity versus integrity should be considered. Mitochondrial markers—such as citrate synthase activity as an enzymatic matrix marker—provide a link to the tissue of origin on the basis of calculating the mitochondrial recovery, *i.e.*, the fraction of mitochondrial marker obtained from a unit mass of tissue. Total mitochondrial protein is frequently applied as a mitochondrial marker, which is restricted to isolated mitochondria.
4. In studies of permeabilized cells, the viability of the cell culture or cell suspension of origin should be reported. Normalization should be evaluated for total cell count or viable cell count.

- 1287 5. Terms and symbols are summarized in **Table 8**. Their use will facilitate transdisciplinary
 1288 communication and support further developments towards a consistent theory of
 1289 bioenergetics and mitochondrial physiology.
 1290 6. Technical terms related to and defined with normal words can be used as index terms in
 1291 databases, support the creation of ontologies towards semantic information processing
 1292 (MitoPedia), and help in communicating analytical findings as impactful data-driven
 1293 stories. ‘*Making data available without making it understandable may be worse than not*
 1294 *making it available at all*’ (National Academies of Sciences, Engineering, and Medicine
 1295 2018). This is a call to carefully contribute to FAIR principles (Findable, Accessible,
 1296 Interoperable, Reusable) for the sharing of scientific data.
 1297

1298 **Table 8. Terms, symbols, and units.**
 1299

1300 Term	1301 Symbol	1302 Unit	1303 Links and comments
1304 alternative quinol oxidase	1305 AOX		1306 Fig. 1
1307 amount of substance B	1308 n_B	1309 [mol]	
1310 cell number	1311 N_{cell}	1312 [x]	1313 Tab. 5; $N_{\text{cell}} = N_{\text{vce}} + N_{\text{dce}}$
1314 cell viability index	1315 CVI		1316 $CVI = N_{\text{vce}}/N_{\text{cell}} = 1 - N_{\text{dce}}/N_{\text{cell}}$
1317 Complexes I to IV	1318 CI to CIV		1319 respiratory ET Complexes; Fig. 1
1320 concentration of substance B	1321 $c_B = n_B \cdot V^{-1}$; [B]	1322 [mol·m ⁻³]	1323 Box 2
1324 dead cell number	1325 N_{dce}	1326 [x]	1327 Tab. 5; non-viable cells, loss of plasma 1328 membrane barrier function
1329 electron transfer system	1330 ETS		1331 Fig. 1, Fig. 4
1332 flow, for substance B	1333 I_B	1334 [mol·s ⁻¹]	1335 system-related extensive quantity; Fig. 6
1336 flux, for substance B	1337 J_B	1338 <i>varies</i>	1339 size-specific quantity; Fig. 6
1340 inorganic phosphate	1341 P_i		1342 Fig. 2
1343 intact cell number, viable cell number	1344 N_{vce}	1345 [x]	1346 Tab. 5; viable cells, intact of plasma 1347 membrane barrier function
1348 LEAK	1349 LEAK		1350 Tab. 1, Fig. 4
1351 mass of sample X	1352 m_X	1353 [kg]	1354 Tab. 4
1355 mass of entity X	1356 M_X	1357 [kg]	1358 mass of object X; Tab. 4
1359 MITOCARTA			1360 https://www.broadinstitute.org/scientific-community/science/programs/metabolic-disease-program/publications/mitocarta/mitocarta-in-0
1361 MitoPedia			1362 http://www.bioblast.at/index.php/MitoPedia
1363 mitochondria or mitochondrial	1364 mt		1365 Box 1
1366 mitochondrial DNA	1367 mtDNA		1368 Box 1
1369 mitochondrial concentration	1370 $C_{\text{mtE}} = \text{mtE} \cdot V^{-1}$	1371 [mtEU·m ⁻³]	1372 Tab. 4
1373 mitochondrial content	1374 $\text{mtE}_X = \text{mtE} \cdot N_X^{-1}$	1375 [mtEU·x ⁻¹]	1376 Tab. 4
1377 mitochondrial elemental unit	1378 mtEU	1379 <i>varies</i>	1380 Tab. 4, specific units for mt-marker
1381 mitochondrial inner membrane	1382 mtIM		1383 MIM is widely used; the first M is 1384 replaced by mt; Box 1
1385 mitochondrial outer membrane	1386 mtOM		1387 MOM is widely used; the first M is 1388 replaced by mt; Box 1
1389 mitochondrial recovery	1390 Y_{mtE}		1391 fraction of <i>mtE</i> recovered in sample 1392 from the tissue of origin
1393 mitochondrial yield	1394 $Y_{\text{mtE}/m}$		1395 $Y_{\text{mtE}/m} = Y_{\text{mtE}} \cdot D_{\text{mtE}}$
1396 negative	1397 neg		1398 Fig. 2
1399 number concentration of X	1400 C_{NX}	1401 [x·m ⁻³]	1402 Tab. 4
1403 number of entities X	1404 N_X	1405 [x]	1406 Tab. 4, Fig. 7
1407 number of entity B	1408 N_B	1409 [x]	1410 Tab. 4
1411 oxidative phosphorylation	1412 OXPHOS		1413 Tab. 1, Fig. 4
1414 oxygen concentration	1415 $c_{\text{O}_2} = n_{\text{O}_2} \cdot V^{-1}$; [O ₂]	1416 [mol·m ⁻³]	1417 Section 3.2
1418 permeabilized cell number	1419 N_{pce}	1420 [x]	1421 Tab. 5; experimental permeabilization 1422 of plasma membrane; $N_{\text{pce}} = N_{\text{cell}}$

1347	phosphorylation of ADP to ATP	P \gg		Section 2.2
1348	positive	pos		Fig. 2
1349	proton in the negative compartment	H ⁺ _{neg}		Fig. 2
1350	proton in the positive compartment	H ⁺ _{pos}		Fig. 2
1351	rate of electron transfer in ET state	<i>E</i>		ET-capacity; Tab. 1
1352	rate of LEAK respiration	<i>L</i>		Tab. 1
1353	rate of oxidative phosphorylation	<i>P</i>		OXPHOS capacity; Tab. 1
1354	rate of residual oxygen consumption	<i>ROx</i>		Tab. 1
1355	residual oxygen consumption	ROX		Tab. 1
1356	respiratory supercomplex	SC I _n III _n IV _n		Box 1; supramolecular assemblies composed of variable copy numbers (<i>n</i>) of CI, CIII and CIV
1357				
1358				
1359	specific mitochondrial density	$D_{mtE} = mtE \cdot m_X^{-1}$	[mtEU·kg ⁻¹]	Tab. 4
1360	volume	<i>V</i>	[m ³]	Tab. 7
1361	weight, dry weight	<i>W_d</i>	[kg]	used as mass of sample <i>X</i> ; Fig. 6
1362	weight, wet weight	<i>W_w</i>	[kg]	used as mass of sample <i>X</i> ; Fig. 6
1363				

1364

1365 Acknowledgements

1366 We thank M. Beno for management assistance. Supported by COST Action CA15203
1367 MitoEAGLE and K-Regio project MitoFit (E.G.).

1368

1369 **Competing financial interests:** E.G. is founder and CEO of Oroboros Instruments, Innsbruck,
1370 Austria.

1371

1372

1373 5. References

1374

1375 Altmann R (1894) Die Elementarorganismen und ihre Beziehungen zu den Zellen. Zweite vermehrte Auflage.
1376 Verlag Von Veit & Comp, Leipzig:160 pp.

1377 Beard DA (2005) A biophysical model of the mitochondrial respiratory system and oxidative phosphorylation.
1378 PLoS Comput Biol 1(4):e36.

1379 Benda C (1898) Weitere Mitteilungen über die Mitochondria. Verh Dtsch Physiol Ges:376-83.

1380 Birkedal R, Laasmaa M, Vendelin M (2014) The location of energetic compartments affects energetic
1381 communication in cardiomyocytes. Front Physiol 5:376.

1382 Breton S, Beaupré HD, Stewart DT, Hoeh WR, Blier PU (2007) The unusual system of doubly uniparental
1383 inheritance of mtDNA: isn't one enough? Trends Genet 23:465-74.

1384 Brown GC (1992) Control of respiration and ATP synthesis in mammalian mitochondria and cells. Biochem J
1385 284:1-13.

1386 Calvo SE, Klauser CR, Mootha VK (2016) MitoCarta2.0: an updated inventory of mammalian mitochondrial
1387 proteins. Nucleic Acids Research 44:D1251-7.

1388 Calvo SE, Julien O, Clauser KR, Shen H, Kamer KJ, Wells JA, Mootha VK (2017) Comparative analysis of
1389 mitochondrial N-termini from mouse, human, and yeast. Mol Cell Proteomics 16:512-23.

1390 Campos JC, Queliconi BB, Bozi LHM, Bechara LRG, Dourado PMM, Andres AM, Jannig PR, Gomes KMS,
1391 Zambelli VO, Rocha-Resende C, Guatimosim S, Brum PC, Mochly-Rosen D, Gottlieb RA, Kowaltowski AJ,
1392 Ferreira JCB (2017) Exercise reestablishes autophagic flux and mitochondrial quality control in heart failure.
1393 Autophagy 13:1304-317.

1394 Canton M, Luvisetto S, Schmehl I, Azzone GF (1995) The nature of mitochondrial respiration and
1395 discrimination between membrane and pump properties. Biochem J 310:477-81.

1396 Chance B, Williams GR (1955a) Respiratory enzymes in oxidative phosphorylation. I. Kinetics of oxygen
1397 utilization. J Biol Chem 217:383-93.

1398 Chance B, Williams GR (1955b) Respiratory enzymes in oxidative phosphorylation: III. The steady state. J Biol
1399 Chem 217:409-27.

1400 Chance B, Williams GR (1955c) Respiratory enzymes in oxidative phosphorylation. IV. The respiratory chain. J
1401 Biol Chem 217:429-38.

1402 Chance B, Williams GR (1956) The respiratory chain and oxidative phosphorylation. Adv Enzymol Relat Subj
1403 Biochem 17:65-134.

1404 Cobb LJ, Lee C, Xiao J, Yen K, Wong RG, Nakamura HK, Mehta HH, Gao Q, Ashur C, Huffman DM, Wan J,
1405 Muzumdar R, Barzilai N, Cohen P (2016) Naturally occurring mitochondrial-derived peptides are age-

- 1406 dependent regulators of apoptosis, insulin sensitivity, and inflammatory markers. *Aging* (Albany NY) 8:796-
1407 809.
- 1408 Cohen ER, Cvitas T, Frey JG, Holmström B, Kuchitsu K, Marquardt R, Mills I, Pavese F, Quack M, Stohner J,
1409 Strauss HL, Takami M, Thor HL (2008) Quantities, units and symbols in physical chemistry, IUPAC Green
1410 Book, 3rd Edition, 2nd Printing, IUPAC & RSC Publishing, Cambridge.
- 1411 Cooper H, Hedges LV, Valentine JC, eds (2009) *The handbook of research synthesis and meta-analysis*. Russell
1412 Sage Foundation.
- 1413 Coopersmith J (2010) Energy, the subtle concept. The discovery of Feynman's blocks from Leibnitz to Einstein.
1414 Oxford University Press:400 pp.
- 1415 Cummins J (1998) Mitochondrial DNA in mammalian reproduction. *Rev Reprod* 3:172-82.
- 1416 Dai Q, Shah AA, Garde RV, Yonish BA, Zhang L, Medvitz NA, Miller SE, Hansen EL, Dunn CN, Price TM
1417 (2013) A truncated progesterone receptor (PR-M) localizes to the mitochondrion and controls cellular
1418 respiration. *Mol Endocrinol* 27:741-53.
- 1419 Divakaruni AS, Brand MD (2011) The regulation and physiology of mitochondrial proton leak. *Physiology*
1420 (Bethesda) 26:192-205.
- 1421 Doerrier C, Garcia-Souza LF, Krumschnabel G, Wohlfarter Y, Mészáros AT, Gnaiger E (2018) High-Resolution
1422 FluoRespirometry and OXPHOS protocols for human cells, permeabilized fibres from small biopsies of
1423 muscle and isolated mitochondria. *Methods Mol. Biol.* (in press)
- 1424 Doskey CM, van 't Erve TJ, Wagner BA, Buettner GR (2015) Moles of a substance per cell is a highly
1425 informative dosing metric in cell culture. *PLOS ONE* 10:e0132572.
- 1426 Drahota Z, Milerová M, Stieglerová A, Houstek J, Ostádal B (2004) Developmental changes of cytochrome *c*
1427 oxidase and citrate synthase in rat heart homogenate. *Physiol Res* 53:119-22.
- 1428 Duarte FV, Palmeira CM, Rolo AP (2014) The role of microRNAs in mitochondria: small players acting wide.
1429 *Genes* (Basel) 5:865-86.
- 1430 Ernster L, Schatz G (1981) Mitochondria: a historical review. *J Cell Biol* 91:227s-55s.
- 1431 Estabrook RW (1967) Mitochondrial respiratory control and the polarographic measurement of ADP:O ratios.
1432 *Methods Enzymol* 10:41-7.
- 1433 Faber C, Zhu ZJ, Castellino S, Wagner DS, Brown RH, Peterson RA, Gates L, Barton J, Bickett M, Hagerty L,
1434 Kimbrough C, Sola M, Bailey D, Jordan H, Elangbam CS (2014) Cardiolipin profiles as a potential
1435 biomarker of mitochondrial health in diet-induced obese mice subjected to exercise, diet-restriction and
1436 ephedrine treatment. *J Appl Toxicol* 34:1122-9.
- 1437 Fell D (1997) *Understanding the control of metabolism*. Portland Press.
- 1438 Garlid KD, Beavis AD, Ratkje SK (1989) On the nature of ion leaks in energy-transducing membranes. *Biochim*
1439 *Biophys Acta* 976:109-20.
- 1440 Garlid KD, Semrad C, Zinchenko V. Does redox slip contribute significantly to mitochondrial respiration? In:
1441 Schuster S, Rigoulet M, Ouhabi R, Mazat J-P, eds (1993) *Modern trends in biothermokinetics*. Plenum Press,
1442 New York, London:287-93.
- 1443 Gerö D, Szabo C (2016) Glucocorticoids suppress mitochondrial oxidant production via upregulation of
1444 uncoupling protein 2 in hyperglycemic endothelial cells. *PLoS One* 11:e0154813.
- 1445 Gnaiger E. Efficiency and power strategies under hypoxia. Is low efficiency at high glycolytic ATP production a
1446 paradox? In: *Surviving Hypoxia: Mechanisms of Control and Adaptation*. Hochachka PW, Lutz PL, Sick T,
1447 Rosenthal M, Van den Thillart G, eds (1993a) CRC Press, Boca Raton, Ann Arbor, London, Tokyo:77-109.
- 1448 Gnaiger E (1993b) Nonequilibrium thermodynamics of energy transformations. *Pure Appl Chem* 65:1983-2002.
- 1449 Gnaiger E (2001) Bioenergetics at low oxygen: dependence of respiration and phosphorylation on oxygen and
1450 adenosine diphosphate supply. *Respir Physiol* 128:277-97.
- 1451 Gnaiger E (2009) Capacity of oxidative phosphorylation in human skeletal muscle. *New perspectives of*
1452 *mitochondrial physiology*. *Int J Biochem Cell Biol* 41:1837-45.
- 1453 Gnaiger E (2014) Mitochondrial pathways and respiratory control. An introduction to OXPHOS analysis. 4th ed.
1454 *Mitochondr Physiol Network* 19.12. Oroboros MiPNet Publications, Innsbruck:80 pp.
- 1455 Gnaiger E, Méndez G, Hand SC (2000) High phosphorylation efficiency and depression of uncoupled respiration
1456 in mitochondria under hypoxia. *Proc Natl Acad Sci USA* 97:11080-5.
- 1457 Greggio C, Jha P, Kulkarni SS, Lagarrigue S, Broskey NT, Boutant M, Wang X, Conde Alonso S, Ofori E,
1458 Auwerx J, Cantó C, Amati F (2017) Enhanced respiratory chain supercomplex formation in response to
1459 exercise in human skeletal muscle. *Cell Metab* 25:301-11.
- 1460 Hinkle PC (2005) P/O ratios of mitochondrial oxidative phosphorylation. *Biochim Biophys Acta* 1706:1-11.
- 1461 Hofstadter DR (1979) Gödel, Escher, Bach: An eternal golden braid. A metaphorical fugue on minds and
1462 machines in the spirit of Lewis Carroll. Harvester Press:499 pp.
- 1463 Illaste A, Laasmaa M, Peterson P, Vendelin M (2012) Analysis of molecular movement reveals latticelike
1464 obstructions to diffusion in heart muscle cells. *Biophys J* 102:739-48.
- 1465 Jasienski M, Bazzaz FA (1999) The fallacy of ratios and the testability of models in biology. *Oikos* 84:321-26.
- 1466 Jepihhina N, Beraud N, Sepp M, Birkedal R, Vendelin M (2011) Permeabilized rat cardiomyocyte response
1467 demonstrates intracellular origin of diffusion obstacles. *Biophys J* 101:2112-21.

- 1468 Klepinin A, Ounpuu L, Guzun R, Chekulayev V, Timohhina N, Tepp K, Shevchuk I, Schlattner U, Kaambre T
 1469 (2016) Simple oxygraphic analysis for the presence of adenylate kinase 1 and 2 in normal and tumor cells. *J*
 1470 *Bioenerg Biomembr* 48:531-48.
- 1471 Klingenberg M (2017) UCP1 - A sophisticated energy valve. *Biochimie* 134:19-27.
- 1472 Koit A, Shevchuk I, Ounpuu L, Klepinin A, Chekulayev V, Timohhina N, Tepp K, Puurand M, Truu L, Heck K,
 1473 Valvere V, Guzun R, Kaambre T (2017) Mitochondrial respiration in human colorectal and breast cancer
 1474 clinical material is regulated differently. *Oxid Med Cell Longev* 1372640.
- 1475 Komlódi T, Tretter L (2017) Methylene blue stimulates substrate-level phosphorylation catalysed by succinyl-
 1476 CoA ligase in the citric acid cycle. *Neuropharmacology* 123:287-98.
- 1477 Lane N (2005) *Power, sex, suicide: mitochondria and the meaning of life*. Oxford University Press:354 pp.
- 1478 Larsen S, Nielsen J, Neigaard Nielsen C, Nielsen LB, Wibrand F, Stride N, Schroder HD, Boushel RC, Helge
 1479 JW, Dela F, Hey-Mogensen M (2012) Biomarkers of mitochondrial content in skeletal muscle of healthy
 1480 young human subjects. *J Physiol* 590:3349-60.
- 1481 Lee C, Zeng J, Drew BG, Sallam T, Martin-Montalvo A, Wan J, Kim SJ, Mehta H, Hevener AL, de Cabo R,
 1482 Cohen P (2015) The mitochondrial-derived peptide MOTS-c promotes metabolic homeostasis and reduces
 1483 obesity and insulin resistance. *Cell Metab* 21:443-54.
- 1484 Lee SR, Kim HK, Song IS, Youm J, Dizon LA, Jeong SH, Ko TH, Heo HJ, Ko KS, Rhee BD, Kim N, Han J
 1485 (2013) Glucocorticoids and their receptors: insights into specific roles in mitochondria. *Prog Biophys Mol*
 1486 *Biol* 112:44-54.
- 1487 Leek BT, Mudaliar SR, Henry R, Mathieu-Costello O, Richardson RS (2001) Effect of acute exercise on citrate
 1488 synthase activity in untrained and trained human skeletal muscle. *Am J Physiol Regul Integr Comp Physiol*
 1489 280:R441-7.
- 1490 Lemieux H, Blier PU, Gnaiger E (2017) Remodeling pathway control of mitochondrial respiratory capacity by
 1491 temperature in mouse heart: electron flow through the Q-junction in permeabilized fibers. *Sci Rep* 7:2840.
- 1492 Lenaz G, Tioli G, Falasca AI, Genova ML (2017) Respiratory supercomplexes in mitochondria. In: *Mechanisms*
 1493 *of primary energy trasduction in biology*. M Wikstrom (ed) Royal Society of Chemistry Publishing, London,
 1494 UK:296-337.
- 1495 Margulis L (1970) *Origin of eukaryotic cells*. New Haven: Yale University Press.
- 1496 Meinild Lundby AK, Jacobs RA, Gehrig S, de Leur J, Hauser M, Bonne TC, Flück D, Dandanell S, Kirk N,
 1497 Kaech A, Ziegler U, Larsen S, Lundby C (2018) Exercise training increases skeletal muscle mitochondrial
 1498 volume density by enlargement of existing mitochondria and not de novo biogenesis. *Acta Physiol* 222,
 1499 e12905.
- 1500 Menshikova EV, Ritov VB, Fairfull L, Ferrell RE, Kelley DE, Goodpaster BH (2006) Effects of exercise on
 1501 mitochondrial content and function in aging human skeletal muscle. *J Gerontol A Biol Sci Med Sci* 61:534-
 1502 40.
- 1503 Menshikova EV, Ritov VB, Ferrell RE, Azuma K, Goodpaster BH, Kelley DE (2007) Characteristics of skeletal
 1504 muscle mitochondrial biogenesis induced by moderate-intensity exercise and weight loss in obesity. *J Appl*
 1505 *Physiol* (1985) 103:21-7.
- 1506 Menshikova EV, Ritov VB, Toledo FG, Ferrell RE, Goodpaster BH, Kelley DE (2005) Effects of weight loss
 1507 and physical activity on skeletal muscle mitochondrial function in obesity. *Am J Physiol Endocrinol Metab*
 1508 288:E818-25.
- 1509 Miller GA (1991) *The science of words*. Scientific American Library New York:276 pp.
- 1510 Mitchell P (1961) Coupling of phosphorylation to electron and hydrogen transfer by a chemi-osmotic type of
 1511 mechanism. *Nature* 191:144-8.
- 1512 Mitchell P (2011) Chemiosmotic coupling in oxidative and photosynthetic phosphorylation. *Biochim Biophys*
 1513 *Acta Bioenergetics* 1807:1507-38.
- 1514 Mogensen M, Sahlin K, Fernström M, Glintborg D, Vind BF, Beck-Nielsen H, Højlund K (2007) Mitochondrial
 1515 respiration is decreased in skeletal muscle of patients with type 2 diabetes. *Diabetes* 56:1592-9.
- 1516 Mohr PJ, Phillips WD (2015) Dimensionless units in the SI. *Metrologia* 52:40-7.
- 1517 Moreno M, Giacco A, Di Munno C, Goglia F (2017) Direct and rapid effects of 3,5-diiodo-L-thyronine (T2).
 1518 *Mol Cell Endocrinol* 7207:30092-8.
- 1519 Morrow RM, Picard M, Derbeneva O, Leipzig J, McManus MJ, Gousspillou G, Barbat-Artigas S, Dos Santos C,
 1520 Hepple RT, Murdock DG, Wallace DC (2017) Mitochondrial energy deficiency leads to hyperproliferation of
 1521 skeletal muscle mitochondria and enhanced insulin sensitivity. *Proc Natl Acad Sci U S A* 114:2705-10.
- 1522 Murley A, Nunnari J (2016) The emerging network of mitochondria-organelle contacts. *Mol Cell* 61:648-53.
- 1523 National Academies of Sciences, Engineering, and Medicine (2018) *International coordination for science data*
 1524 *infrastructure: Proceedings of a workshop—in brief*. Washington, DC: The National Academies Press. doi:
 1525 <https://doi.org/10.17226/25015>.
- 1526 Paradies G, Paradies V, De Benedictis V, Ruggiero FM, Petrosillo G (2014) Functional role of cardiolipin in
 1527 mitochondrial bioenergetics. *Biochim Biophys Acta* 1837:408-17.
- 1528 Pesta D, Gnaiger E (2012) High-Resolution Respirometry. OXPHOS protocols for human cells and
 1529 permeabilized fibres from small biopsies of human muscle. *Methods Mol Biol* 810:25-58.

- 1530 Pesta D, Hoppel F, Macek C, Messner H, Faulhaber M, Kobel C, Parson W, Burtscher M, Schocke M, Gnaiger
 1531 E (2011) Similar qualitative and quantitative changes of mitochondrial respiration following strength and
 1532 endurance training in normoxia and hypoxia in sedentary humans. *Am J Physiol Regul Integr Comp Physiol*
 1533 301:R1078–87.
- 1534 Price TM, Dai Q (2015) The role of a mitochondrial progesterone receptor (PR-M) in progesterone action.
 1535 *Semin Reprod Med* 33:185-94.
- 1536 Puchowicz MA, Varnes ME, Cohen BH, Friedman NR, Kerr DS, Hoppel CL (2004) Oxidative phosphorylation
 1537 analysis: assessing the integrated functional activity of human skeletal muscle mitochondria – case studies.
 1538 *Mitochondrion* 4:377-85. Puntschart A, Claassen H, Jostarndt K, Hoppeler H, Billeter R (1995) mRNAs of
 1539 enzymes involved in energy metabolism and mtDNA are increased in endurance-trained athletes. *Am J*
 1540 *Physiol* 269:C619-25.
- 1541 Quiros PM, Mottis A, Auwerx J (2016) Mitonuclear communication in homeostasis and stress. *Nat Rev Mol*
 1542 *Cell Biol* 17:213-26.
- 1543 Rackham O, Mercer TR, Filipovska A (2012) The human mitochondrial transcriptome and the RNA-binding
 1544 proteins that regulate its expression. *WIREs RNA* 3:675–95.
- 1545 Reichmann H, Hoppeler H, Mathieu-Costello O, von Bergen F, Pette D (1985) Biochemical and ultrastructural
 1546 changes of skeletal muscle mitochondria after chronic electrical stimulation in rabbits. *Pflugers Arch* 404:1-
 1547 9.
- 1548 Renner K, Amberger A, Konwalinka G, Gnaiger E (2003) Changes of mitochondrial respiration, mitochondrial
 1549 content and cell size after induction of apoptosis in leukemia cells. *Biochim Biophys Acta* 1642:115-23.
- 1550 Rich P (2003) Chemiosmotic coupling: The cost of living. *Nature* 421:583.
- 1551 Rostovtseva TK, Sheldon KL, Hassanzadeh E, Monge C, Saks V, Bezrukov SM, Sackett DL (2008) Tubulin
 1552 binding blocks mitochondrial voltage-dependent anion channel and regulates respiration. *Proc Natl Acad Sci*
 1553 *USA* 105:18746-51.
- 1554 Rustin P, Parfait B, Chretien D, Bourgeron T, Djouadi F, Bastin J, Rötig A, Munnich A (1996) Fluxes of
 1555 nicotinamide adenine dinucleotides through mitochondrial membranes in human cultured cells. *J Biol Chem*
 1556 271:14785-90.
- 1557 Saks VA, Veksler VI, Kuznetsov AV, Kay L, Sikk P, Tiivel T, Tranqui L, Olivares J, Winkler K, Wiedemann F,
 1558 Kunz WS (1998) Permeabilised cell and skinned fiber techniques in studies of mitochondrial function in
 1559 vivo. *Mol Cell Biochem* 184:81-100.
- 1560 Salabei JK, Gibb AA, Hill BG (2014) Comprehensive measurement of respiratory activity in permeabilized cells
 1561 using extracellular flux analysis. *Nat Protoc* 9:421-38.
- 1562 Sazanov LA (2015) A giant molecular proton pump: structure and mechanism of respiratory complex I. *Nat Rev*
 1563 *Mol Cell Biol* 16:375-88.
- 1564 Schneider TD (2006) Claude Shannon: biologist. The founder of information theory used biology to formulate
 1565 the channel capacity. *IEEE Eng Med Biol Mag* 25:30-3.
- 1566 Schönfeld P, Dymkowska D, Wojtczak L (2009) Acyl-CoA-induced generation of reactive oxygen species in
 1567 mitochondrial preparations is due to the presence of peroxisomes. *Free Radic Biol Med* 47:503-9.
- 1568 Schultz J, Wiesner RJ (2000) Proliferation of mitochondria in chronically stimulated rabbit skeletal muscle--
 1569 transcription of mitochondrial genes and copy number of mitochondrial DNA. *J Bioenerg Biomembr* 32:627-
 1570 34.
- 1571 Simson P, Jephthina N, Laasmaa M, Peterson P, Birkedal R, Vendelin M (2016) Restricted ADP movement in
 1572 cardiomyocytes: Cytosolic diffusion obstacles are complemented with a small number of open mitochondrial
 1573 voltage-dependent anion channels. *J Mol Cell Cardiol* 97:197-203.
- 1574 Stucki JW, Ineichen EA (1974) Energy dissipation by calcium recycling and the efficiency of calcium transport
 1575 in rat-liver mitochondria. *Eur J Biochem* 48:365-75.
- 1576 Tonkonogi M, Harris B, Sahlin K (1997) Increased activity of citrate synthase in human skeletal muscle after a
 1577 single bout of prolonged exercise. *Acta Physiol Scand* 161:435-6.
- 1578 Waczulikova I, Habodaszova D, Cagalinec M, Ferko M, Ulicna O, Mateasik A, Sikurova L, Ziegelhöffer A
 1579 (2007) Mitochondrial membrane fluidity, potential, and calcium transients in the myocardium from acute
 1580 diabetic rats. *Can J Physiol Pharmacol* 85:372-81.
- 1581 Wagner BA, Venkataraman S, Buettner GR (2011) The rate of oxygen utilization by cells. *Free Radic Biol Med*
 1582 51:700-712.
- 1583 Wang H, Hiatt WR, Barstow TJ, Brass EP (1999) Relationships between muscle mitochondrial DNA content,
 1584 mitochondrial enzyme activity and oxidative capacity in man: alterations with disease. *Eur J Appl Physiol*
 1585 *Occup Physiol* 80:22-7.
- 1586 Watt IN, Montgomery MG, Runswick MJ, Leslie AG, Walker JE (2010) Bioenergetic cost of making an
 1587 adenosine triphosphate molecule in animal mitochondria. *Proc Natl Acad Sci U S A* 107:16823-7.
- 1588 Weibel ER, Hoppeler H (2005) Exercise-induced maximal metabolic rate scales with muscle aerobic capacity. *J*
 1589 *Exp Biol* 208:1635–44.
- 1590 White DJ, Wolff JN, Pierson M, Gemmell NJ (2008) Revealing the hidden complexities of mtDNA inheritance.
 1591 *Mol Ecol* 17:4925–42.

- 1592 Wikström M, Hummer G (2012) Stoichiometry of proton translocation by respiratory complex I and its
1593 mechanistic implications. *Proc Natl Acad Sci U S A* 109:4431-6.
- 1594 Willis WT, Jackman MR, Messer JI, Kuzmiak-Glancy S, Glancy B (2016) A simple hydraulic analog model of
1595 oxidative phosphorylation. *Med Sci Sports Exerc* 48:990-1000.